AD-A210 193

OFFICE OF NAVAL RESEARCH

Contract N00014-86-K-0556

Technical Report No. 86

Solvent Dynamical Effects in Electron Transfer: Predicted Influences of Electron Coupling upon the Rate-Dielectric Friction Dependence

by

A. Gochev, G. E. McManis, and M. J. Weaver

Prepared for Publication

in the

Journal of Chemical Physics

Purdue University

Department of Chemistry

West Lafayette, Indiana 47907

DTIC
ELECTE
JUL 18 1989
S D
E

July 1, 1989

Reproduction in whole, or in part, is permitted for any purpose of the United States Government.

* This document has been approved for public release and sale: its distribution is unlimited.

89 7 18 026

CURITY CLASSIFICATION OF THIS PAGE

REPORT DOCUMENTATION PAGE

a REPORT SECURITY CLASSIFICATION Unclassified	1b RESTRICTIVE MARKINGS
a SECURITY CLASSIFICATION AUTHORITY	3 DISTRIBUTION / AVAILABILITY OF REPORT Approved for public release and sale; its distribution is unlimited.
b DECLASSIFICATION / DOWNGRADING SCHEDULE	
PERFORMING ORGANIZATION REPORT NUMBER(S) Technical Report No. 86	5 MONITORING ORGANIZATION REPORT NUMBER(S)
a NAME OF PERFORMING ORGANIZATION Purdue University Department of Chemistry 6b OFFICE SYMBOL (If applicable)	7a NAME OF MONITORING ORGANIZATION Division of Sponsored Programs Purdue Research Foundation
c ADDRESS (City, State, and ZIP Code) Purdue University Department of Chemistry West Lafayette, Indiana 47907	7b ADDRESS (City, State, and ZIP Code) Purdue University West Lafayette, Indiana 47907
a NAME OF FUNDING / SPONSORING ORGANIZATION Office of Naval Research 8b OFFICE SYMBOL (If applicable)	9 PROCUREMENT INSTRUMENT IDENTIFICATION NUMBER Contract No. N00014-86-K-0556
c ADDRESS (City, State, and ZIP Code) 800 N. Quincy Street Arlington, VA 22217	10 SOURCE OF FUNDING NUMBERS PROGRAM ELEMENT NO / PROJECT NO / TASK NO / WORK UNIT ACCESSION NO

1 TITLE (Include Security Classification)
Solvent Dynamical Effects in Electron Transfer: Predicted Influences of Electron Coupling upon the Rate-Dielectric Friction Dependence

2 PERSONAL AUTHOR(S)
A. Gochev, G. E. McManis, and M. J. Weaver

13a TYPE OF REPORT	13b TIME COVERED	14 DATE OF REPORT (Year, Month, Day)	15 PAGE COUNT
Technical	FROM 10/1/87 TO 6/30/89	July 1, 1989	

16 SUPPLEMENTARY NOTATION

17 COSATI CODES		
FIELD	GROUP	SUB-GROUP
		sub gr

18 SUBJECT TERMS (Continue on reverse if necessary and identify by block number)
outer-sphere electron exchange, Debye solvents, "encounter preequilibrium" treatment
1/5

19 ABSTRACT (Continue on reverse if necessary and identify by block number)
Tau sub L

The predicted dependence of the bimolecular rate constant for outer-sphere electron exchange, k_{ex}, upon the longitudinal relaxation time, τ_L, for Debye solvents is examined numerically on the basis of a suitably combined rate formulation in order to examine the manner and extent to which the rate-solvent friction dependence, of particular experimental significance, should be sensitive to the degree of donor-acceptor electronic coupling and related factors. The treatment accounts for the contributions to k_{ex} from a spatial distribution of reactant pairs as well as for the effects of donor-acceptor interactions upon the unimolecular rate constant, k_{et} (s^{-1}), for each encounter geometry. The latter include the influence of electronic interactions as prescribed by the matrix coupling element, H_{12}, upon the effective frequency for adiabatic barrier crossing, ν_n, as well as upon the electronic transmission coefficient, κ_{el} (i.e. the degree of reaction nonadiabaticity). The anticipated dependence of the free-energy barrier, as well as ν_n and κ_{el}, upon the donor-acceptor
(continued on back)

sub gr sub el

20 DISTRIBUTION / AVAILABILITY OF ABSTRACT	21 ABSTRACT SECURITY CLASSIFICATION
☒ UNCLASSIFIED/UNLIMITED ☒ SAME AS RPT ☐ DTIC USERS	
22a NAME OF RESPONSIBLE INDIVIDUAL	22b TELEPHONE (Include Area Code) / 22c OFFICE SYMBOL

D FORM 1473, 84 MAR 83 APR edition may be used until exhausted
All other editions are obsolete

SECURITY CLASSIFICATION OF THIS PAGE

DTIC
C
INSP

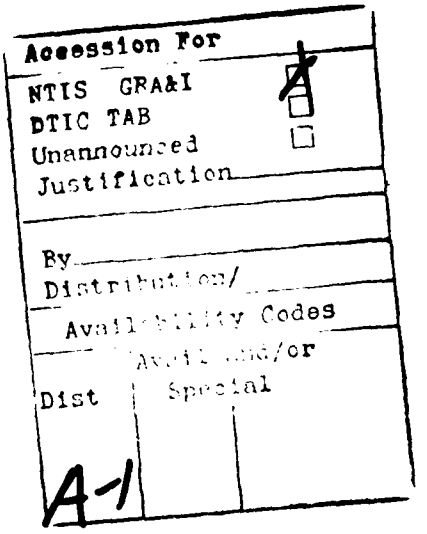

19. (cont.)
separation is accounted for in the k_{ex} calculations. The form of the resulting log k_{ex} - log τ_L^{-1} plots exhibit, as expected, a marked dependence on the value of H_{12} for reactant contact, H_{12}. Over the τ_L^{-1} range appropriate for common solvents at ambient temperatures, ca 1 x 10^{11} to 5 x 10^{12} s^{-1}, the log k_{ex} - log τ_L^{-1} slopes, x, are significantly (or substantially) below unity for $H_{12}^{\circ} \lesssim 0.5$ kcal mol^{-1}; x decreases markedly with increasing τ_L^{-1} and/or for decreasing H_{12}°. The approach to the solvent inertial limit (for large τ_L^{-1}) also tends to decrease x further. Numerical comparisons are made with corresponding log k_{ex} - log τ_L^{-1} plots obtained using the simple "encounter preequilibrium" treatment which presumes that only a fixed narrow range of encounter-pair geometries contribute to k_{ex}. While the form of the plots are not greatly different, the latter more sophisticated treatment generally yields smaller slopes. Some corresponding numerical calculations for electrochemical-exchange reactions are also included.

Solvent Dynamical Effects in Electron Transfer: Predicted Influences of Electronic Coupling upon the Rate-Dielectric Friction Dependence

Alexander Gochev, George E. McManis, and

Michael J. Weaver

Department of Chemistry

Purdue University

West Lafayette, Indiana 47907, USA

J. Chem. Phys.

Submitted November 10, 1988

Revised March 20, 1989

ABSTRACT

The predicted dependence of the bimolecular rate constant for outer-sphere electron exchange, k_{ex}, upon the longitudinal relaxation time, τ_L, for Debye solvents is examined numerically on the basis of a suitably combined rate formulation in order to examine the manner and extent to which the rate-solvent friction dependence, of particular experimental significance, should be sensitive to the degree of donor-acceptor electronic coupling and related factors. The treatment accounts for the contributions to k_{ex} from a spatial distribution of reactant pairs as well as for the effects of donor-acceptor interactions upon the unimolecular rate constant, k_{et} (s^{-1}), for each encounter geometry. The latter include the influence of electronic interactions as prescribed by the matrix coupling element, H_{12}, upon the effective frequency for adiabatic barrier crossing, ν_n, as well as upon the electronic transmission coefficient, κ_{el} (i.e. the degree of reaction nonadiabaticity). The anticipated dependence of the free-energy barrier, as well as ν_n and κ_{el}, upon the donor-acceptor separation is accounted for in the k_{ex} calculations. The form of the resulting log k_{ex} - log τ_L^{-1} plots exhibit, as expected, a marked dependence on the value of H_{12} for reactant contact, H_{12}^o. Over the τ_L^{-1} range appropriate for common solvents at ambient temperatures, ca 1×10^{11} to 5×10^{12} s^{-1}, the log k_{ex} - log τ_L^{-1} slopes, x, are significantly (or substantially) below unity for $H_{12}^o \leq 0.5$ kcal mol^{-1}; x decreases markedly with increasing τ_L^{-1} and/or for decreasing H_{12}^o. The approach to the solvent inertial limit (for large τ_L^{-1}) also tends to decrease x further. Numerical comparisons are made with corresponding log k_{ex} - log τ_L^{-1} plots obtained using the simple "encounter preequilibrium" treatment which presumes that only a fixed narrow range of encounter-pair geometries contribute to k_{ex}. While the form of the plots are not greatly different, the latter more sophisticated treatment generally yields smaller slopes. Some corresponding numerical calculations for electrochemical-exchange reactions are also included.

There are extensive developments occurring at the present time in our understanding of solvent dynamical factors in electron transfer, as for other condensed-phase processes.[1] The original treatments for electron transfer[2] predict that the barrier-crossing frequency for adiabatic processes, ν_n, should simply be proportional to the inverse of the longitudinal solvent relaxation time, τ_L. Subsequent theoretical treatments have included the effects of barrier-top curvature,[3] non-Debye solvent relaxation,[4-7] and reactant vibrational distortions,[8] all within the dielectric continuum limit, as well as solvent molecularity effects by employing the mean spherical approximation.[9]

Most experimental kinetic investigations of these effects involve examining the dependence of the rate parameters for bimolecular homogeneous-phase or electrochemical electron-exchange reactions on the solvent, a range of media being chosen so to provide a suitably large variation in the solvent dynamics.[10,11] After appropriate correction for the solvent-dependent barrier height, the dependence of the electron-exchange rate constant, k_{ex}, (or the inferred barrier-crossing frequency, ν_n) upon τ_L^{-1} or related solvent dynamical parameters can yield substantial insight into the role of solvent friction upon the kinetics.[11] In order for such solvent-friction effects to be manifested, however, it is necessary for the processes to remain essentially adiabatic (or nearly so) within the range of nuclear frequencies accessed by the solvent relaxation dynamics. We recently presented numerical calculations of the dependence of ν_n upon τ_L^{-1} for outer-sphere electron-exchange processes having varying degrees of donor-acceptor orbital overlap as described by the electronic coupling matrix element, H_{12}.[12] For simplicity, the calculations assumed

Debye overdamped relaxation, the effects of reaction nonadiabaticity being accounted for on the basis of a generalized Landau-Zener treatment. The results indicate that substantial H_{12} values, $H_{12} \geq 0.1$ kcal mol^{-1}, are required to maintain reaction adiabaticity and hence preserve the full effect of solvent friction, as τ_L^{-1} is increased within the range ca 3×10^{10} to 3×10^{12} s^{-1} expected for common polar solvents at ambient temperatures.[12]

The calculations presented in ref. 12 were concerned primarily with the solvent frictional dependence of the "local" unimolecular rate constant, k_{et}, referring to a particular geometry of the donor-acceptor pair. Such results can be transposed to yield corresponding information for experimental bimolecular (or electrochemical) rate constants, k_{ex}, most simply by utilizing the so-called "encounter preequilibrium" treatment.[13] This approach presumes that electron transfer takes place over a sufficiently narrow range of precursor-complex geometries such that k_{ex} can be identified approximately with k_{et} multiplied by a "precursor stability constant" K_p. However, the encounter preequilibrium treatment is inherently only an approximation to a more rigorous description of k_{ex} involving an integration of k_{et} over a distribution of reactant separation distances, r.[14] As alluded to recently by Beretan and Onuchic,[15] and as outlined in detailed fashion herein, the relative r-dependent k_{et} contributions to k_{ex} are inexorably altered somewhat as the solvent friction is modified (i.e. τ_L^{-1} is varied) for a given reaction. As a consequence, the predicted dependence of k_{ex} upon τ_L^{-1} deduced using this spatial integration approach may differ significantly from that obtained from the simple encounter preequilibrium formalism that utilizes a constant (i.e. friction-independent) K_p term.

Given the central importance of solvent-dependent friction effects upon k_{ex} to the interpretation of the experimental kinetics,[10,11] it is crucial to elucidate how the effects of electronic coupling combine with solvent friction to determine k_{ex} and, especially, its dependence upon τ_L^{-1}. The objective of the present report is to outline in detail a unified treatment of such combined electronic coupling-solvent friction effects within the Debye continuum approximation that is applicable directly to such experimental systems, and to illustrate its application by means of representative numerical calculations. While attention is focused primarily on homogeneous-phase reactions, some pertinent results are included for electrochemical exchange processes. We present in a companion paper a substantive experimental application of the present solvent friction-dependent analysis, so to provide a novel means of extracting H_{12} values for simple self-exchange reactions.[11g]

THEORETICAL TREATMENT

Bimolecular Rate Formulations

As noted above, the overall measured rate constant for bimolecular electron-exchange reactions in homogeneous solution, k_{ex}, strictly is composed of an integral of "local" unimolecular rate constants, $k_{et}(r)$. Thus we can write[14]

$$k_{ex} = \frac{4\pi N}{10^3} \int_{r_o}^{\infty} r^2 \, k_{et}(r) \, g_{DA}(r) \, dr \qquad (1)$$

where N is Avogadro's number, r_o is the donor-acceptor distance corresponding to the (spherical) reactant's closest approach, and $g_{DA}(r)$ is the radial pair distribution function. For simplicity, $g_{DA}(r)$ is taken

here as unity. The relation corresponding to Eq. (1) that describes electrochemical rate constants, k°_{ex}, is

$$k^{\circ}_{ex} = \int_{r_o}^{\infty} k_{et}(r)\, g_{DA}(r)\, dr \qquad (2)$$

reflecting the linear rather than spherical spatial coordinates relevant to heterogeneous process.[13c]

The local rate constant $k_{et}(r)$ can generally be expressed as[13]

$$k_{et} = \kappa_{el}\nu_n \exp(-\beta\Delta G^*) \qquad (3)$$

where $\beta = (k_B T)^{-1}$ and ΔG^* is the free energy of activation. The electronic transmission coefficient κ_{el} describes the extent to which the effective barrier-crossing frequency falls below the nuclear frequency factor ν_n as a consequence of reaction nonadiabaticity. The effect of solvent friction is manifested entirely in the ν_n term, in that ν_n increases as the solvent friction (most simply τ_L) decreases.

All three components of k_{et} in Eq. (3): κ_{el}, ν_n, and ΔG^*; are expected to depend upon the reactant separation distance r. The electronic matrix coupling element H_{12} will decrease markedly with increasing r, which is usually approximated by the exponential form:[16,17]

$$(H_{12})^2 = (H^{\circ}_{12})^2 \exp[-\alpha(r - r_o)] \qquad (4)$$

where H°_{12} is the matrix coupling element corresponding to $r = r_o$. The coefficient α is usually calculated (or measured) to be in the range ca 1.0 to 1.5 $Å^{-1}$.[16-18]

The dependence of κ_{el} upon r depends on the magnitude of H°_{12} as well as that of α. For reactions where H°_{12} is sufficiently large so that

reaction adiabaticity is achieved, $\kappa_{el} = 1$ for $r = r_o$. As r is increased beyond r_o, however, H_{12} must fall eventually to the point where electron transfer becomes nonadiabatic (i.e. $\kappa_{el} < 1$), whereby the Fermi Golden rule applies, i.e. $\kappa_{el} \propto (H_{12})^2$ (vide infra).[17] Under such nonadiabatic conditions, however, κ_{el} will also depend upon ν_n; for $\kappa_{el} \ll 1$, eventually $\kappa_{el} \propto \nu_n^{-1}$ so that the net preexponential factor $\kappa_{el}\nu_n$ becomes independent of variations in the solvent friction.[12]

The decrease in H_{12} with increasing r will also obviously influence ΔG^* since[19]

$$\Delta G^* = \Delta G_c^* - H_{12} \tag{5}$$

where ΔG_c^* is the barrier for $H_{12} \to 0$, i.e. when the barrier top resembles a cusp. In addition, ΔG^* is expected to increase sharply with increasing r even in the absence of such "resonance splitting" since according to the dielectric continuum treatment of outer-shell barriers:[20]

$$\Delta G_c^* = (e^2/4)(\epsilon_{op}^{-1} - \epsilon_o^{-1})(a^{-1} - r^{-1}) \tag{6}$$

where e is the electronic charge, ϵ_{op} and ϵ_o are the optical and static (zero-frequency) dielectric constants, and a is the reactant radius. The functional dependence of ΔG_c^* upon r^{-1}, predicted by Eq. (6), is in accord with experimental energies of optical electron transfer within mixed-valence complexes having varying internuclear separations r.[21]

The relation corresponding to Eq. (6) for electrochemical reactions is[20]

$$\Delta G_c^* = (e^2/8)(\epsilon_{op}^{-1} - \epsilon_o^{-1})[(a^{-1} - (2r_e)^{-1}] \tag{6a}$$

where r_e is the distance between the reactant and the surface plane. Since outer-sphere processes are often anticipated to occur at the outer Helmholtz plane where the reactant is separated from the metal surface by a solvent monolayer, the influence of the "imaging" term r_e upon ΔG_c^* could be unimportant,[11b,c] yielding only mild increases in ΔG_c^* with increasing r_e.

In the presence of solvent friction, ν_n is anticipated to depend on the barrier height[2-4] as well as on the shape of the barrier top, and hence upon H_{12}.[2-4] Although both these dependencies are relatively mild,[3,12,22] since ν_n tends to increase both with increasing ΔG_c^* and decreasing H_{12} one can predict that ν_n will increase monotonically with increasing r. In the transition-state theory (TST) limit (i.e. in the absence of solvent friction), however, both these lependencies will disappear. In any case, the influence of these factors upon the k_{et}-r profile are overshadowed by the corresponding increases in ΔG^* and decreases in κ_{el} with increasing r, so that $k_{et}(r)$ will inexorably decrease sharply with increasing reactant separation.

Provided that $k_{et}(r)$ declines sufficiently rapidly, to a first approximation the integral in Eq. (1) can be reexpressed simply in the "encounter preequilibrium" formulation[13] as

$$k_{ex} = K_p\, k_{et} = K_p\, \kappa_{el}\, \nu_n \exp(-\beta \Delta G^*) \qquad (7)$$

The preequilibrium constant K_p reflects the spatial range over which significant contributions to k_{ex} occur, with k_{et} and its component parameters κ_{el}, ν_n, and ΔG^* being approximated by the local values at $r = r_o$. However, as noted above it is preferable for the present purposes to perform a spatial k_{ex} integration to find k_{ex} since K_p is expected to change somewhat as the solvent friction is altered (vide infra).

In the sections that follow, we outline a simple combined treatment of the above effects upon $k_{et}(r)$, followed by illustrative numerical predictions of the resulting dependence of k_{ex} upon solvent friction.

The Unimolecular Rate Constant

We require here a treatment of $k_{et}(r)$ which accounts for the alterations in H_{12} and ΔG^* needed for the complete spatial integration in Eq. (1), together with the ability to consider wide variations in the extent of solvent friction. Considered first is a suitable means of describing barrier shape effects upon ν_n, followed by a formalism which can account additionally for nonadiabaticity.

In the presence of solvent friction, as H_{12} increases and the barrier top becomes increasingly rounded the frequency of successful barrier crossings is progressively diminished. This effect, first considered by Kramers,[23] has also been described recently in the context of electron-transfer processes.[3,4,12] In our previous examination of ν_n - solvent friction dependencies,[12] we employed the Smoluchowski treatment described by Calef and Wolynes.[3] This approach describes the passage across the potential-energy surface in terms of simple diffusion. More generally, the diffusion coefficient, D, can be considered to depend on the position, q, along the reaction coordinate potential-energy surface, V(q).[24,25] Whereas D will be independent of q for a pair of harmonic surfaces forming a cusp barrier, when $H_{12} > 0$ the diffusion coefficient within the intersection region, D_b, will differ from that within the parabolic wells, D_w. Indeed, for large H_{12} values (i.e. for large resonance splittings), the D_b component dominates the overall barrier-crossing rate.[24]

An expression for the adiabatic unimolecular rate constant, k^a_{et}, due to Okuyama and Oxtoby is[24]

$$(k^a_{et})^{-1} = 2\int_{-\infty}^{q^*} dq[D(q)\ P_{eq}(q)]^{-1}[\int_{-\infty}^{q} dq'\ P_{eq}(q')]^2 \qquad (8)$$

where $$P_{eq}(q) = Z \exp[-\beta\ V(q)] \qquad (8a)$$

and $$Z = \int_{-\infty}^{\infty} \exp[-\beta\ V(q)]\ dq \approx (2\pi/\beta m\omega_o^2)^{1/2} \qquad (8b)$$

(The approximation in Eq. (8b) arises since the greatest contribution to the integral will be close to the initial state where $V(q) = 0.5\ m\ \omega_o^2\ q^2$.) The value of q is taken to be zero for the reactant initial state; q^* refers to the transition state; m is the "effective mass" of the reacting particle, and ω_o is the well frequency. The above integrals may also be simplified for large barriers ($\beta\Delta G^* \gtrsim 5$) to yield:

$$(k^a_{et})^{-1} \approx 2\int_{o}^{q^*} dq[D(q)\ P_{eq}(q)]^{-1} \qquad (9)$$

Equation (9) is adequate for the numerical calculations presented below, where $\beta\Delta G^* \sim 10$. This relation reduces to the simple Kramers relation[23] (e.g. ref. 3) if D is independent of q; it also can be related directly[24] to the well-known Grote-Hynes result.[1a]

In order to apply this treatment to solvent friction in electron transfer, we require appropriate expressions for both V(q) and D(q). The former can be expressed as[12,19]

$$V(q) = 0.5[V_1(q) + V_2(q)] - 0.5([V_1(q) - V_2(q)]^2 + 4H_{12}^2)^{1/2} \qquad (10)$$

where V_1 and V_2 refer to the reactant and product potential-energy curves,

respectively. These quantities can be expressed in terms of energetic (E) as well as position (q) coordinates. Thus $V_1(q) = 0.5\ m\ \omega_o^2\ q^2$, whereas $V_1(E) = 0.5\ m_E\ \omega_o^2\ E^2$, where $m_E = (2E_r\ \omega_o^2)^{-1}$. Convenient expressions for V_1 and V_2 in the latter (energy) coordinates are

$$V_1(E) = E^2/4E_r;\ V_2(E) = (E - 2E_r)^2/4E_r \tag{11}$$

where E_r is the reorganization energy ($= 4\Delta G^*$ for a symmetric barrier as considered here).

When $H_{12} > 0$, the barrier top can often be approximated by an inverted parabola, allowing the potential-energy surface close to the transition region to be expressed as

$$V_b(E) = \Delta G^* - 0.5\ m_E\ \omega_b^2(E - E_r)^2 \tag{12}$$

where the "characteristic barrier-top" frequency ω_b is related to the well frequency for symmetric barriers by[22,26]

$$\omega_b/\omega_o = [(2\Delta G_c^*/H_{12}) - 1]^{1/2} \tag{13}$$

Given this form of V(E), a general expression for the position-dependent diffusion coefficient can be written as (see Appendix A):

$$D_p(p = w,b) = (\beta\ m_E\ \eta_p^{eff})^{-1} \tag{14}$$

where η_p^{eff} is the effective friction. This quantity can be expressed for Debye solvents as (Appendix A):

$$\eta_w^{eff} = 2\omega_o^2/\eta(1 - [1 - (4\omega_o^2/\eta^2)]^{1/2}) \qquad (\text{for } \eta \geq 2\omega_o) \tag{15a}$$

or

$$\eta_w^{eff} = 2\omega_o^2/\eta \qquad (\text{for } \eta < 2\omega_o) \tag{15b}$$

$$\eta_b^{eff} = 2\omega_b^2/\eta\{[1 + (4\omega_b^2/\eta^2)]^{1/2} - 1]\} \quad (16)$$

where $\eta = \omega_o^2 \tau_L$. Equations (14)-(16) enable D_w and D_b, and hence k_{et}^a, to be determined in terms of τ_L, ω_o, H_{12}, and ΔG^* which together describe the experimental reactant-solvent system. The calculation of k_{et}^a by this means employs D_w for potential energies $E \leq E_s$ and D_b for $E > E_s$, where E_s defines the energy where the well potential surface gives way to the inverted parabola characteristic of the barrier top. This approach therefore provides a relatively general as well as convenient means of accounting for such "barrier-top roundedness", caused by moderate or large electronic coupling, within the adiabatic limit.

As noted above, the effects of electronically nonadiabatic barrier crossing also need to be accounted for, not only in the k_{et}-r integration to find k_{ex} in a given solvent [Eq. (1)] but also so to provide a more complete description of the k_{ex} - τ_L^{-1} dependence. Whereas k_{et}^a is predicted to be proportional to τ_L^{-1} in the absence of solvent inertial effects (i.e. for overdamped solvent motion),[3] k_{et} will fall below k_{et}^a for small H_{12} and/or large τ_L^{-1} and eventually will become independent of τ_L^{-1}.[12]. One means of bridging these two regimes is to regard the overall unimolecular reaction to be composed of separable rate constants for approaching and then crossing the barrier top, so that[2a,4,5,14a]

$$(k_{et})^{-1} = (k_{et}^a)^{-1} + (k_{et}^b)^{-1} \quad (17)$$

where k_{et}^b accounts for the possible influence of reaction nonadiabaticity (i.e. transitions to the upper diabatic surface, rather than adiabatic barrier crossings involving electron transfer). The effect of solvent

friction is contained wholly within k_{et}^{a}.

A significant limitation, however, of Eq. (17) for the present purposes is that it is strictly valid only for sufficiently small "barrier-top roundedness" (small H_{12}) so that k_{et}^{a} is dominated by motion within the potential-energy wells rather than in the intersection region (vide infra). Equation (17) therefore cannot account for the effects of barrier-top shape upon k_{et}^{a}. [Note that a relation of apparently similar form to Eq. (17) has been used to formulate such barrier-shape effects upon k_{et} within the adiabatic limit,[4] where the first term refers to motion within the wells and the second describes the barrier-crossing step (see also ref. 22).] An expression for the "barrier-crossing" rate constant, k_{et}^{b}, valid at least in the normal (as opposed to inverted) free-energy regime[27] as considered here is

$$k_{et}^{b} = \tilde{\kappa}_{el}\, k^{TST} = \tilde{\kappa}_{el}(\omega_o/2\pi)\, \exp(-\beta\Delta G^{*}) \tag{18}$$

where k^{TST} denotes the rate constant in the TST limit, and $\tilde{\kappa}_{el}$ (not to be confused with the overall electronic transmission coefficient κ_{el} employed above) can be expressed as[28]

$$\tilde{\kappa}_{el} = \int_{o}^{\infty} W_{el}(E_1)\, \exp(-\beta E_1)\, d(\beta E_1) \tag{19}$$

where

$$W_{el} = [1 - \exp(-2\pi\gamma)]/[1 - 0.5\, \exp(-2\pi\gamma)] \tag{19a}$$

$$\gamma = |H_{12}|^{2}/2\hbar\omega_o(E_r E_1)^{1/2} \tag{19b}$$

and $E_1 (= E - \Delta G^{*})$ is the system energy relative to that at the barrier peak.

As shown in Appendix B, $\tilde{\kappa}_{el}$ can be expressed to a good approximation more simply as:

$$\tilde{\kappa}_{el} = 4\pi^{3/2}\gamma_T/(1 + 4\pi^{3/2}\gamma_T) \tag{20}$$

where[19]
$$\gamma_T = |H_{12}|^2/2\hbar\ \omega_o(E_r\ k_BT)^{1/2} \tag{20a}$$

Another, more familiar, form for $\tilde{\kappa}_{el}$ is[13a,14a] (See Appendix B):

$$\tilde{\kappa}_{el} \simeq \frac{2\ \bar{W}_{LZ}}{1 + \bar{W}_{LZ}} = \frac{2[1 - \exp(-2\pi^{3/2}\gamma_T)]}{2 - \exp(-2\pi^{3/2}\gamma_T)} \tag{21}$$

where $\bar{W}_{LZ}$ [= 1 - $\exp(-2\pi^{3/2}\gamma_T)$] is the averaged Landau-Zener probability for a "single crossing" of the barrier top. Equation (21) is obtained as an approximation to Eq. (19) by replacing the γ term in W_{el} [Eq. (19a)] by its average value $\pi^{3/2}\gamma_T$.

From Eqs. (17) and (18) we can express the distance-dependent unimolecular rate constant $k_{et}(r)$ as

$$k_{et}(r) = \frac{\tilde{\kappa}_{el}\ k^{TST}}{1 + [\tilde{\kappa}_{el}\ k^{TST}/k^a_{et}]} \tag{22}$$

A closely related simplified expression for k_{et} resulting from Eqs. (17) and (20), utilized previously, is[2a,4,15]

$$k_{et} = \frac{2\pi\ |H_{12}|^2(16\hbar^2\ \pi\ \Delta G^*_c\ \beta^{-1})^{-1/2}\ \exp(-\beta\Delta G^*)}{1 + (\pi\ |H_{12}|^2\ \tau_L/\hbar\ \Delta G^*_c)} \tag{23}$$

This relation is derived from Eq. (17) by assuming that k^a_{et} refers to overdamped solvent motion over a cusp barrier (i.e. $H_{12} \to 0$), whereupon[2-4]

$$k^a_{et} = \tau_L^{-1}\ (\beta\Delta G^*/4\pi)^{1/2}\ \exp(-\beta\Delta G^*_c) \tag{24}$$

and $H_{12} \ll k_B T$ so that the expression for k_{et}^{na} reduces to[29]

$$k_{et}^{na} = 2\pi \, |H_{12}|^2 \, \hbar^{-1} (16\pi \Delta G^* \beta^{-1})^{-\frac{1}{2}} \exp(-\beta \Delta G_c^*) \tag{25}$$

$$= 4\pi^{3/2} \, \gamma_T \, k^{TST} \tag{25a}$$

Although Eq. (23) as well as Eq. (22) provides a useful approximate form under conditions where H_{12} is small, it does not account either for the influence of the barrier-top curvature upon ν_n or for the onset of the inertial limit, where $\nu_n \to \omega_o/2\pi$ (vide infra). These shortcomings may be avoided by using in place of Eq. (17) the following modified interpolation expression, obtained by Straub and Berne[30] [Eq. 3.15 of ref. 30a], which can be written as

$$(k_{et})^{-1} = (k_{et}^a)^{-1} + \left(\frac{1 - \bar{W}_{LZ}}{2\bar{W}_{LZ}}\right) (k^{TST})^{-1} \tag{26}$$

By assuming the relation between $\tilde{\kappa}_{el}$ and $\bar{W}_{LZ}$ given in Eq. (21), and rearranging, we obtain

$$k_{et} = \frac{\tilde{\kappa}_{el} k^{TST}}{1 - \tilde{\kappa}_{el} + [\tilde{\kappa}_{el} k^{TST}/k_{et}^a]} \tag{27}$$

Equation (27) differs from the simplified Eq. (22) by the presence of an additional $-\tilde{\kappa}_{el}$ term in the denominator. The two expressions will therefore only become equivalent either when $\tilde{\kappa}_{el} \ll 1$ and/or when $k^{TST}/k_{et}^a \gg 1$; i.e. for small H_{12} and/or high friction. Equation (27) is clearly preferred for the present purposes since it should be applicable also to systems having large H_{12} values, a situation often encountered[11g] and indeed required in order for solvent dynamical effects to influence k_{et}

in low friction media (vide supra).[12] A related point is that Eq. (27), unlike Eq. (22), yields the correct prefactor, $\omega_o/2\pi$, in the adiabatic "zero-friction" (i.e. TST) limit. [Equation (22) yields a prefactor that is twofold smaller in this limit.]

Equation (27) therefore describes in a straightforward as well as general fashion the separate effects of reaction nonadiabaticity and solvent friction via the $\tilde{\kappa}_{el}$ and k^a_{et} terms, respectively. The influence of solvent inertia appears in both k^{TST} and k^a_{et}. If the reaction involves sufficient electronic coupling to be entirely adiabatic, then $k_{et} = k^a_{et}$ in the presence of solvent friction, or $k_{et} = k^{TST}$ in its absence. Even though Eq. (27) is utilized primarily in the following numerical calculations, we also include some results obtained with the conventional simplified formula Eq. (23) for comparative purposes.

The form of the preceding parameters can readily be related to the phenomenological quantities κ_{el} and ν_n in Eq. (3). The latter parameter is obtained directly from k^a_{et} [Eq. (9)] by removing the Boltzmann term since [cf Eq. (3)]:

$$k^a_{et} = \nu_n \exp(-\beta\Delta G^*) \tag{28}$$

The transmission coefficient κ_{el} can be identified with the more familiar quantity $\tilde{\kappa}_{el}$ in the TST limit where solvent friction disappears such that $2\pi\nu_n = \omega_o$. In the presence of friction, $\kappa_{el} > \tilde{\kappa}_{el}$; from Eqs. (3) and (28) κ_{el} can be expressed simply as $\kappa_{el} = k_{et}/k^a_{et}$. A general relation between κ_{el} and $\tilde{\kappa}_{el}$ can be obtained simply from Eqs. (21) and (25):

$$\kappa_{el} = \tilde{\kappa}_{el}/[\kappa_a + \tilde{\kappa}_{el}(1 - \kappa_a)] \tag{29}$$

where the "adiabatic transmission coefficient" κ_a (= k^a_{et}/k^{TST}) describes the influence of solvent friction upon k_{et} in the absence of reaction nonadiabaticity. In some earlier calculations,[12] we accounted for the combined effects of friction and nonadiabaticity upon k_{et} by using a modified form of Eq. (21) expressed in terms of κ_{el} rather than $\tilde{\kappa}_{el}$. The numerical similarities of these treatments are noted briefly in Appendix B.

NUMERICAL RESULTS AND DISCUSSION

Homogeneous Bimolecular Reactions

Having outlined a relatively versatile means of predicting the functional k_{ex}-τ_L^{-1} dependence, at least in the continuum Debye limit, it is of primary interest to examine the extent to which this solvent-friction dependence is sensitive to the fundamental kinetic parameters involved, and especially to the extent of donor-acceptor orbital overlap, H^o_{12}.

Figure 1 displays an illustrative set of log k_{ex}-log τ_L^{-1} plots for homogeneous bimolecular processes obtained using the conventional simplified expression for k_{et} [Eq. (23)] along with Eqs. (1), (4)-(6), for the sequence of H^o_{12} values 0.02, 0.05, 0.1, 0.2, 0.5, and 1.0 kcal mol^{-1}. (The k_{ex} values at a given τ_L value increase with increasing H_{12}.) The other parameters required in this analysis were held constant as follows: ΔG^*_c = 5.0 kcal mol^{-1}, α = 1.25 $Å^{-1}$, r_o = 2a = 8 Å and T = 298 K. These values are probably typical for many experimental systems.[11,16,18] Choosing different values of α and r_o, at least within the ranges normally expected experimentally (ca 0.8 to 1.5 $Å^{-1}$ and 3 to 6 Å, respectively) have relatively little influence on the form of these plots. Admittedly, the larger H_{12} values chosen violate the assumption $H_{12} \ll k_BT$ that is embodied

in Eq. (23); it is nevertheless still instructive to examine the influence of altering H_{12} more widely upon the predicted k_{ex}-τ_L^{-1} dependence. Figure 1 shows that while approximately $k_{ex} \propto \tau_L^{-1}$ at relatively small τ_L^{-1} values, as expected, increasing τ_L^{-1} leads eventually to marked decreases in the log k_{ex}-log τ_L^{-1} slope and eventually to a solvent friction-independent rate in accordance with the Fermi Golden Rule, whereupon $k_{ex} \propto H_{12}^{o}$. Necessarily, then, the range of τ_L^{-1} values where these deviations occur shift markedly upwards as H_{12}^{o} is increased; i.e. solvent friction effects persist to larger ν_n values. Even for τ_L and/or H_{12}^{o} values that are sufficiently large so that essentially $k_{ex} \propto \tau_L^{-1}$, k_{ex} is seen to increase significantly with increasing H_{12}^{o}. This is due to the corresponding decreases in the effective barrier height [Eq. (5)].

Figures 2A & B display corresponding sets of log k_{ex}-log τ_L^{-1} plots obtained by utilizing the more complete k_{et} expression [Eq. (27)], including the effects of barrier-top roundedness upon k_{et}. These calculations utilized the same input parameter values as in Fig. 1, but with inertial limiting (i.e. TST) frequencies, $\omega_o/2\pi$, of 1 x 10^{12} and 5 x 10^{12} s^{-1} in Figs. 2A and B, respectively. (These values represent typical rough lower and upper limits of $\omega_o/2\pi$ for simple polar solvents.[22]) As before, k_{ex} was calculated from $k_{et}(r)$ using Eqs. (1), (4)-(6), with $k_{et}^{a}(r)$ obtained using Eqs. (8)-(16), $\tilde{\kappa}_{el}$ from Eq. (20) and k^{TST} from Eq. (18). The evaluation of k_{ex} in this manner therefore involves a double integration, both spatially [Eq. (1)] and along the reaction coordinate [Eq. (8)]. The double integrals were evaluated using a standard two-dimensional quadrature technique,[31] executed on the Purdue University Cyber 205 supercomputer using double precision (128 bit). [The single integral

calculations, for example in Fig. 1, were undertaken using a Zenith 387 laboratory microcomputer with 64 bit precision at 16 MHz.]

The overall shapes of the log k_{ex} - log τ_L^{-1} plots in Figs. 2A and B do not differ greatly from those in Fig. 1, indicating that the inclusion of the effects of barrier-top curvature and solvent inertia do not have a dramatic effect on the rate-solvent friction dependence under most conditions. Nevertheless, the influence of the latter factor is clearly seen in the traces in Figs. 2A and B for the highest H_{12} values (i.e. for the strongest electronic coupling) in that the plots deviate from linearity for large τ_L^{-1} values to a greater extent as ω_o is decreased (compare Fig. 2A versus 2B). This behavior reflects the approach to the inertial limiting rate as the solvent friction is reduced to small values (i.e. when $\tau_L^{-1} \geq \omega_o$).[32] However, in some experimental systems this "inertial limit" may not be observable,[1a,23] in part due to the well-known onset of diffusion control.[33] The primary influence of barrier-top roundedness is to diminish the displacements between the log k_{ex} - log τ_L^{-1} curves in the "adiabatic" region, corresponding to large τ_L (i.e. high friction), where roughly $k_{et} \propto \tau_L^{-1}$ (compare Figs. 2A,B with Fig. 1). This effect arises because the inclusion of barrier-top roundedness (i.e. deviations from a cusp) tends to depress ν_n, and therefore k_{et} and k_{ex}, increasingly as H_{12}^o and hence the extent of this curvature increases (vide supra).

One significant feature of both Figs. 1 and 2 is that the slopes of the log k_{ex}-log τ_L^{-1} plots are significantly below unity even within the relatively high friction, "adiabatic", region. Even for strong electronic coupling, say when H_{12}^o = 1 kcal mol^{-1} (i.e. the uppermost trace in these figures), the log k_{ex} - log τ_L^{-1} slopes increase slightly with decreasing

τ_L^{-1}. For example, for the trace where H_{12}° = 1 kcal mol^{-1} in Fig. 2B, the slope increases from 0.93 for $\tau_L^{-1} = 10^{11}$ s^{-1} to 0.98 for $\tau_L^{-1} = 10^{8}$ s^{-1}. Although the degree of nonlinearity can be relatively minor (as in this example), it reflects in part the changes in the form of the k_{et}-r distribution [i.e. the integrand in Eq. (1)] as the extent of solvent friction is altered (cf ref. 15).

Given this effect, it is of interest to compare more closely such log k_{ex} - log τ_L^{-1} plots obtained by performing a spatial k_{et} integration [i.e. using Eq. (1)] with corresponding curves resulting from the simplified "encounter preequilibrium" treatment [Eq. (7)]. Figure 3 contains a pair of comparisons of this type for representative H_{12}° values of 0.05 and 0.5 kcal mol^{-1}. In both cases, the solid traces were extracted from Fig. 2B, i.e. involving a spatial k_{et} integration and including the effects of both barrier-top roundedness and solvent inertia. The dotted traces were taken from Fig. 1, i.e. with only spatial k_{et} integration taken into account. (The numerical parameters used in Fig. 3 are identical to those in Figs. 1 and 2B.) The corresponding dashed curves in Fig. 3, on the other hand, include the effects of barrier-top roundedness and solvent inertia as for the solid traces, but k_{ex} was derived from k_{et} by employing Eq. (7) rather than using the spatial integration procedure. The k_{et} values used to calculate k_{ex} from Eq. (7) refer to the values with the reactants essentially in contact, i.e. with $r = r_o$, with K_p taken as 0.25 $\underline{M}^{-1}$. This latter value, although somewhat arbitrary, corresponds to that expected for r_o (= 2a) = 8 Å, with an effective "reaction zone thickness" of about 0.5 Å.[11b,d] Since K_p is presumed to be independent of both τ_L^{-1} and H_{12}° in this simple analysis, the form of the resulting

log k_{ex} - log τ_L^{-1} curves (dashed traces in Fig. 3) will reflect only the friction-dependent behavior of the unimolecular rate constant k_{et} for the reactants in contact (cf calculations in ref. 12).

Although in some respects similar, this trio of plots for both H_{12}° = 0.05 and 0.5 kcal mol^{-1} (lower and upper sets, respectively, in Fig. 3) show subtle yet significant differences. In particular, the curves calculated using the spatial k_{et} integration (solid, dotted traces) exhibit significantly greater nonlinearities as well as smaller slopes than that obtained from the simple preequilibrium treatment. Given that the τ_L^{-1} values for simple polar solvents at ambient temperatures differ by only about 50 fold (or less), within the range ca 1 x 10^{11} to 5 x 10^{12} s^{-1},[11c,d] inspection of Figs. 1-3 shows that sub-unit log k_{ex} - log τ_L^{-1} slopes (i.e. the fractional power law $k_{ex} \propto \tau_L^{-x}$, where $0 < x < 1$) might often be anticipated experimentally. The average value of x should depend both on the magnitude of H_{12}° and the range of τ_L values accessed (cf. ref. 6b). The presence of solvent inertial effects, anticipated for low-friction solvents, may also act to depress these slopes somewhat, especially since ω_o is anticipated to vary with the solvent in a qualitatively similar fashion, albeit to a markedly smaller extent than τ_L^{-1}.[22]

Interestingly, log k_{ex} - log τ_L^{-1} (or related) plots having similarly fractional slopes have been predicted on the basis of other considerations, such as the influence of reactant vibrational distortions[8] and to the presence of additional high-frequency solvent relaxation.[22] The experimental observation of such a "fractional power-law" rate-τ_L^{-1} dependence in at least one case[10f] has been attributed to the former factor.[8] It would, however, seem at least as likely that this observation

is actually due to the friction-dependent emergence of nonadiabatic effects, as considered here. In any case, it is evident that such fractional log k_{ex} - log τ_L^{-1} dependencies should often be expected. This is especially true given the likelihood that many outer-sphere electron-transfer reactions involve relatively weak donor-acceptor orbital overlap, such that $H_{12}^{o} \leq 0.1$ to 0.2 kcal mol^{-1}.[4a,16]

In order to investigate more closely the role of the k_{et}-r functionality upon the predicted k_{ex}-τ_L^{-1} curves it is also instructive to examine the dependence of k_{et} upon r for varying degrees of solvent friction and orbital overlap. Figures 4A and B contain plots of k_{et} ratioed to the value when $r = r_o$ (i.e. reactant spheres in contact), k_{et}/k_{et}^{o}, against the radial separation distance, $(r - r_o)$. The rate constants were calculated as in Fig. 2B, thereby accounting both for barrier-top roundedness and solvent inertial effects. The four traces shown in both Figs. 4A and B refer to H_{12}^{o} values of 0.02, 0.2, 0.5 and 1.0 kcal mol^{-1}, as indicated. The τ_L values in Figs. 4A and B are held constant at 5×10^{-8} s and 5×10^{-12} s, respectively. Although somewhat arbitrary, these τ_L values are chosen so to correspond to conditions where the reaction remains entirely adiabatic (at $r = r_o$) over the entire range of H_{12}^{o} values selected (Fig. 4A), and where the reaction switches from essentially nonadiabatic to adiabatic behavior as H_{12}^{o} is increased (Fig. 4B). Differences in these (k_{et}/k_{et}^{o}) - r profiles as H_{12}^{o} is varied reflect variations in the relative spatial-dependent contributions to the overall integration yielding k_{ex} [Eq. (1)].

In the adiabatic case (Fig. 4A), the form of this (k_{et}/k_{et}^{o})-r dependence is seen to depend only to a small extent upon H_{12}^{o}. The slightly

more pronounced decrease in k_{et}/k^{o}_{et} with increasing r for larger H^{o}_{12} values is due primarily to the concomitant increases in ΔG^{*} caused by the spatial variations in H_{12}. Slightly greater alterations in the (k_{et}/k^{o}_{et})-r profiles with increasing H^{o}_{12} are seen in Fig. 4B, in that the shallowness of the descent with increasing r is maximized at an intermediate H^{o}_{12} value, 0.2 kcal mol^{-1}. This nonmonotonic behavior is due to the competing influences of the H_{12}-r dependence upon κ_{el} and ΔG^{*}; only the latter factor influences the profiles in Fig. 4A. In any case, no dramatic changes in these profiles with varying H^{o}_{12} (or τ_{L}) are seen in either Fig. 4A or B.

This relative invariance of the shape of the (k_{et}/k^{o}_{et})-r profiles is responsible for the approximate applicability of the simple encounter preequilibrium treatment in the present context, since then the effective value of K_{p} will not vary greatly with either H^{o}_{12} or τ_{L}. This perhaps fortunate situation is brought about in part by the increases in ΔG^{*} with r predicted from Eq. (5) and especially Eq. (6). In order to illustrate this point, a set of (k_{et}/k^{o}_{et})-r curves, corresponding to the conditions of Fig. 4A except that ΔG^{*}_{c} is taken to be *independent* of r, are shown in Fig. 5. In contrast to Fig. 4A, the (k_{et}/k^{o}_{et})-r profiles in Fig. 5 extend to substantially larger r values and are much more dependent upon H^{o}_{12}. These differences graphically demonstrate the importance of the anticipated spatial dependencies of ΔG^{*} to the integral in Eq. (1).

As already noted, Beretan and Onuchic have recently considered in detail some factors that influence the form of the bimolecular rate expression and its dependence on solvent friction in the intermediate regime between the adiabatic and nonadiabatic limits.[15] Included in ref. 15 is a discussion of some assumptions embodied in the well-known

spatial integration formula for k_{ex} [Eq. (1)].[15b] In essence, their analysis utilizes a relation similar to Eq. (23) so that no explicit consideration of barrier-shape effects upon k^e_{et} are included; as noted above this expression is valid only for $H_{12} \ll k_BT$. The present results also differ from those in ref. 15 in that the numerically important effects of spatial variations in ΔG^* are not contained in the latter.

Electrochemical Reactions

Although the foregoing analysis applied to electrochemical reactions proceeds along the same lines as for bimolecular processes, the form of the resulting log k_{ex} - log τ_L^{-1} plots can be significantly different. This is not only because of the differing form of the spatial k_{et} integration [Eq. (2) versus Eq. (1)] but also in view of the milder dependence of ΔG_c^* upon the donor-acceptor separation in the electrochemical case (vide supra).

Figure 6 shows typical plots of log k^e_{ex} versus log τ_L^{-1} obtained for conditions corresponding to those in Fig. 3, but where the ΔG^*-r dependence is given by Eq. (6a) and the k_{et}-r integration utilizes Eq. (2). As before, the solid and dotted curves refer to the presence and absence, respectively, of the effects of barrier-top roundedness and solvent inertia. The distance of closest approach is taken as 8 Å, with ΔG_c^* for infinite surface-reactant separation (i.e. $r_e \rightarrow \infty$) set at 5 kcal mol^{-1}. (These values are typical for some experimental systems.[11c]) The corresponding dashed curves in Fig. 6 were obtained from the encounter preequilibrium treatment as in Fig. 3, but with K_p taken as 0.5 Å (cf refs. 11b, 13c). As before, the lower and upper trio of curves (displaced as

such at large τ_L^{-1}) refer to H_{12}° values (i.e. H_{12} at r_e = 8 Å) of 0.05 and 0.5 kcal mol^{-1}.

Close comparison of Fig. 6 with Fig. 3 shows that the τ_L-dependent log k_{ex} - log τ_L^{-1} slopes for the corresponding electrochemical and homogeneous curves calculated using k_{et} spatial integration are very similar (within ca 5%), being smaller than the slopes for the companion "encounter preequilibrium" curves to a comparable extent. This result might at first sight appear surprising, since the presumed increases in ΔG^* with increasing r are milder in the electrochemical case, yielding k_{et}-r profiles which extend to larger r and exhibit a greater sensitivity to τ_L^{-1} than for the homogeneous-phase case (vide supra). Offsetting this factor is the involvement of linear spatial coordinates in the electrochemical k_{et}-r integration rather than spherical coordinates as in the homogeneous-phase case. In comparison with the latter, the former function is weighted more heavily towards rate contributions for smaller donor-acceptor separations.[34]

Overall, then, similar log k_{ex} - log τ_L^{-1} dependencies might often be anticipated for electrochemical and homogeneous-phase exchange processes. Differences can nevertheless be expected, especially since the values of H_{12} and their functional dependence upon r may be quite dissimilar in the two environments.[35,36] Another complication for electrochemical process is that the dependence of ΔG_c^* upon r_e may be quite different to that predicted by the simple imaging expression Eq. (6a).[37]

Concluding Remarks

It should be recognized that the assumptions embodied in the foregoing

analysis impart to it less than general applicability. In particular, the barrier-crossing frequency may often be influenced importantly by inner-shell as well as solvent reorganization dynamics. The analysis will also need to be modified for reactions having large driving forces, and where electrostatic work terms are present since they can alter substantially the form of $k_{et}(r)$. These complications will nevertheless be absent for homogeneous self-exchange processes where one of the reacting partners is uncharged. This circumstance prevails in the experimental companion paper to the present work.[11g] Even in the absence of such work terms, however, the assumptions that g_{DA} is independent of r, and that H_{12} remains constant when the solvent is varied may prove to be significant weaknesses once specific solvation effects upon the approach of the reaction partners are considered. The desirability of including the effects of reactant orientation upon the H_{12}-separation distance profiles is also clear.[16,38] On the other hand, the predicted rate-friction dependencies are not particularly sensitive to most details of the kinetic model for k_{et}, such as the form of $\tilde{\kappa}_{el}$ used, the r-dependence of H_{12}, and the modifications to k^a_{et} caused by barrier-top shape effects.

The effect of non-Debye relaxation, which appear to exert marked influences upon k_{ex} in a number of solvents,[10e,11c,d] can be incorporated into the numerical treatment.[22] However, given the magnitude of this effect together with complications in its physical description[22] the analysis of combined electronic coupling-solvent friction factors is perhaps most prudently restricted to Debye-like media. Deviations from the dielectric continuum approximation, manifested most simply in spatial variations in τ_L, can also be considered, although on the basis of a mean

spherical approximation (MSA) treatment[9] the influence upon k_{ex} can be relatively small.[39]

Given that most outer-sphere electron-transfer processes are likely to involve relatively weak or moderate degrees of electronic coupling, however, the present treatment should provide not only a useful means of describing the effects of varying the solvent friction, but also can yield valuable information on the magnitude of H_{12} itself. Just such an application from our laboratory, to the self-exchange kinetics of various cobalt and iron metallocenes, is presented elsewhere.[11g]

Acknowledgments

Professors D. W. Oxtoby and J. T. Hynes provided valuable advice concerning adiabatic rate expressions. We are also grateful to Dr. David Beratan for helpful discussions. This work is supported by the Office of Naval Research.

Appendix A

As noted in the text, we utilize the treatment for adiabatic barrier crossing described by Okuyama and Oxtoby,[24] involving the concept of a position-dependent diffusion coefficient, D_p. This requires the calculation of a pair of diffusion coefficients, D_w and D_b, which describe the passage of the system sequentially up the reactant well (for $E \leq E_s$) and over the barrier top ($E_s < E \leq E_r$), respectively. Outlined here is the derivation of Eqs. (15) and (16), which express D_w and D_b in terms of the effective friction η_w^{eff} and η_b^{eff}, respectively [Eq. (14)]. The problem involves the calculation of η_w^{eff} and η_b^{eff} for two Brownian oscillators with natural frequencies ω_o and ω_b acted on by external forces $-dV_1/dE$ and $-dV_b/dE$, respectively. We use the results of refs. 24 and 25 derived on the basis of the Generalized Langevin equation (GLE) for Brownian oscillators and, more specifically, the Generalized Smoluchowski equation for the corresponding GLE.

The diffusion coefficient D_p is defined as the long time limit of $D_p(t)$, expressed in terms of the position autocorrelation function $\chi_p(t) = \langle E(t)\, E(o)\rangle_p / \langle [E(o)]^2 \rangle_p$:

$$D_p = \lim_{t \to \infty} D_p(t) = \lim_{t \to \infty} (\beta m_E \omega_p^2)^{-1} [\pm\, d \ln \chi_p(t)/dt] = (\beta m_E \eta_p^{eff})^{-1} \qquad (A.1)$$

where the plus and minus signs are approximate for p = b and p = w, respectively.

Since we are concerned here only with Debye solvents, the friction η is independent of frequency and equal to $\omega_o^2 \tau_L$ (e.g. ref. 4), whereby $\chi_w(t)$ and $\chi_b(t)$ are determined by the inverse Laplace transforms:

$$\chi_w(t) = \mathcal{L}^{-1} \{(s + \eta)/(s^2 + \eta s + \omega_o^2)\} \qquad (A.2)$$

$$\chi_b(t) = \mathcal{L}^{-1} \{(s + \eta)/s^2 + \eta s \cdot \omega_b^2)\} \qquad (A.3)$$

The solutions $\chi_p(t)$ can be written in the general form:

$$\chi_p(t) = A_{1p} \exp(S_{1p}t) + A_{2p} \exp(S_{2p}t) \tag{A.4}$$

where S_{1p} and S_{2p} are the roots of the quadratic equations in the denominators of Eqs. (A.2) and (A.3) for p = w and p = b, respectively, and

$$\begin{aligned} A_{1p} &= (S_{1p} + \eta)/(S_{1p} - S_{2p}) \\ A_{2p} &= (S_{2p} + \eta)/(S_{2p} - S_{1p}) \end{aligned} \tag{A.5}$$

The correlation function $\chi_p(t)$ for the "instability region" $V_b(q)$ is determined by the positive real root[24,25] $S_{1b} = [(\eta^2 + 4\omega_b^2)^{1/2} - (\eta)]/2$. Inserting $\chi_b(t)$ [$= A_{1b} \exp(S_{1b}t)$] into Eq. (A.1) yields $D_b = S_{1b}/\beta m_E \omega_b^2$, leading to Eq. (16).

For the overdamped and critically damped friction regimes ($\eta \geq 2\omega_o$), $\chi_w(t)$ is determined by the two negative roots $S_{2w} \leq S_{1w} \leq 0$[24a] and its long-time behavior is determined by the larger root S_{1w}, i.e. only by the first term in Eq. (A.4). Inserting again $\chi_w(t)$ into Eq. (A.1) yields $D_w = (-S_{1w})/\beta m_E \omega_o^2$, giving Eq. (15a).

For the underdamped regime ($\eta < 2\omega_o$), we obtain two conjugate roots $S_{1w} = S_{2w}^* = a_w + ib_w$; also $A_{1w} = A_{2w}^* = x + iy$. Thus:[24a]

$$\chi_w(t) = 2(x^2 + y^2)^{1/2} \exp(a_w t) \cos(\varphi + b_w t) \tag{A.6}$$

and

$$D_w(t) = (\beta m_E \omega_o^2)^{-1}[-a_w + b_w \mathrm{tg}(\varphi + b_w t)] \tag{A.7}$$

with $\varphi = \mathrm{arctg}\ (y/x)$. The long time behavior of $D_w(t)$ can be considered to be dominated by $-(\beta m_E \omega_o^2)^{-1} a_w$ due to the oscillatory character of the tg-term. Making this approximation,[24a] we obtain Eq. (15b).

It is also of interest to examine the forms of Eqs. (15) and (16) in

the limiting case where motion in both the well and the barrier-top regions are overdamped, i.e. when $\eta >> \omega_o$ and $\eta >> \omega_b$, respectively. In this case, the square root terms in both Eq. (15a) and (16) can be approximated as $(1 \pm x^2)^{1/2} \simeq 1 - 0.5x^2$, where $x = 2\omega_o/\eta$ or $2\omega_b/\eta$, respectively, reduces these relations simply to $\eta_w^{eff} = \eta_b^{eff} = \eta$. This limiting case corresponds to the Kramers diffusion treatment generalized to allow for barrier-top curvature,[3] which we utilized for the numerical calculations in ref. 12.

Appendix B

Considered here is a justification of the form of $\bar{\kappa}_{el}$ [Eq. (20)] employed in the above analysis.

We can generally express k_{et} in the form [cf Eq. (21)]

$$k_{et} = \frac{k_{et}^{na}}{1 + (k_{et}^{na}/k_{et}^{a})} = \frac{\Omega}{1 + \Omega} \nu_n \exp(-\beta\Delta G^*) \qquad (B.1)$$

From Eqs. (24) and (25), the "adiabaticity criterion" Ω ($= k_{et}^{na}/k_{et}^{a}$) is for $H_{12} << k_B T$ [i.e. where Eq. (B.1) reduces to Eq. (23)]:

$$\Omega = 4\pi |H_{12}|^2 \hbar^{-1} E_r^{-1} \tau_L \qquad (B.2)$$

since [cf Eqs. (24),(25)]:

$$\nu_n = \tau_L^{-1}(\beta\Delta G^*/4\pi)^{1/2} \qquad (B.3)$$

Combining Eq. (B.1) with Eq. (3) yields

$$\kappa_{el} = \Omega/(1 + \Omega) \qquad (B.4)$$

The well-known form of γ_T[19] [Eq. (20a)], suggests the use of the related quantity γ_ℓ:

$$\gamma_f = |H_{12}|^2/4\hbar\ \pi\ \nu_n\ (E_r\ k_B T)^{\frac{1}{2}} \qquad (B.5)$$

where ω_o is replaced by $2\pi\ \nu_n$ in order to allow for the presence of solvent friction (cf ref. 40). From Eqs. (B.2) and B.5) we obtain $\Omega = 4\pi^{3/2}\gamma_f$; from Eq. (B.4) we can express κ_{el} as

$$\kappa_{el} = 4\pi^{3/2}\ \gamma_f/(1 + 4\pi^{3/2}\ \gamma_f) \qquad (B.6)$$

The form of Eq. (B.6) suggests intuitively the corresponding expression [Eq. (20)] for $\tilde{\kappa}_{el}$ given in the text.

The form of Eq. (B.5), and its TST analog Eq. (20), although approximate, provides a useful means of interpolating between the adiabatic and nonadiabatic limits. Table B1 contains a numerical comparison between values of $\tilde{\kappa}_{el}$ evaluated for typical values of ω_o and H_{12} (at $\Delta G^* = 6$ kcal mol^{-1}) using the approximate form Eq. (20) and the exact expression Eq. (19). Also included in Table B1 are corresponding $\tilde{\kappa}_{el}$ values obtained using the oft-encountered multiple-crossing expression,[13a,14a] Eq. (21). Inspection of Table B.1 shows that Eq. (20) provides a generally better approximation than Eq. (21) to the exact κ_{el} expression Eq. (19), although the differences are not large. The preference for such a Padé form for κ_{el}, as in Eq. (20), has also been noted elsewhere.[6b]

This numerical success of Eq. (20) also underscores the general usefulness of Eq. (B.6). Thus in the presence of friction, Eq. (B.6) becomes equivalent to the transmission coefficient extracted by inserting Eqs. (23) and (B.3) for k_{et} and ν_n, respectively, into Eq. (3). In the absence of friction, Eq. (B.6) reduces to Eq. (20). Equation (B.6) therefore provides a useful approximate means of accounting in a combined manner for the effects of friction and reaction nonadiabaticity. A related

approach, involving the use of Eq. (21) with $\omega_o/2\pi$ replaced by $2\pi\nu_n$, was utilized in our earlier numerical calculations of rate-friction dependencies.[12,41]

TABLE B1. Numerical Comparisons of the Electronic Transmission Coefficient $\tilde{\kappa}_{el}$ Evaluated using Different Expressions for 6.0 kcal mol^{-1} barrier at 298 K.

H_{12}, kcal mol^{-1}	0.6	0.2	0.2	0.1	0.1	0.05	0.01
$\omega_o/2\pi$, s^{-1}	10^{13}	10^{13}	10^{12}	10^{13}	19^{12}	10^{10}	10^{9}
$\tilde{\kappa}_{el}$ [Eq. (19)]	0.504	0.103	0.540	0.029	0.219	0.945	0.785
$\tilde{\kappa}_{el}$ [Eq. (20)]	0.520	0.110	0.553	0.030	0.236	0.885	0.756
$\tilde{\kappa}_{el}$ [Eq. (21)]	0.590	0.113	0.631	0.030	0.250	0.989	0.881

References

1. For example, see (a) J. T. Hynes, in "Theory of Chemical Reaction Dynamics", M. Baer, ed., CRC Press, Boca Raton, FL, Vol. IV, 1985, Chapter 4; (b) J. T. Hynes, J. Stat. Phys., 42, 149 (1986); (c) D. Chandler, J. Stat. Phys., 42, 49 (1986).

2. (a) L. D. Zusman, Chem. Phys., 49, 295 (1980); (b) B. T. Yakobson, A. I. Burschtein, Chem. Phys., 49, 385 (1980); (c) I. V. Alexandrov, Chem. Phys., 51, 499 (1980).

3. D. F. Calef, P. G. Wolynes, J. Phys. Chem., 87, 3387 (1983).

4. J. T. Hynes, J. Phys. Chem., 90, 3701 (1986).

5. I. Rips, J. Jortner, J. Chem. Phys., 87, 2090 (1987).

6. (a) M. Sparpaglione, S. Mukamel, J. Phys. Chem., 91, 3938 (1987); (b) M. Sparpaglione, S. Mukamel, J. Chem. Phys., 88, 3263 (1988); (c) M. Sparpaglione, S. Mukamel, J. Chem. Phys., 88, 4300 (1988).

7. L. D. Zusman, Chem. Phys., 119, 51 (1988).

8. (a) H. Sumi, R. A. Marcus, J. Chem. Phys., 84, 4894 (1986); (b) W. Nadler, R. A. Marcus, J. Chem. Phys., 86, 3906 (1987).

9. (a) P. G. Wolynes, J. Chem. Phys., 86, 5133 (1987); (b) I. Rips, J. Klafter, J. Jortner, J. Chem. Phys., 88, 3246 (1988).

10. (a) A. Kapturkiewicz, B. Behr, J. Electroanal. Chem., 179, 187 (1984); (b) W. Harrer, G. Grampp, W. Jaenicke, Chem. Phys. Lett., 112, 263 (1984); (c) A. Kapturkiewicz, M. Opallo, J. Electroanal. Chem., 185, 15 (1985); (d) M. Opallo, A. Kapturkiewicz, Electrochim. Acta, 30, 1301 (1985); (e) M. Opallo, J. Chem. Soc. Far. Trans. I, 82, 339 (1986); (f) M. McGuire, G. McLendon, J. Phys. Chem., 90, 2547 (1986).

11. (a) M. J. Weaver, T. Gennett, Chem. Phys. Lett., 113, 213 (1985); (b) T. Gennett, D. F. Milner, M. J. Weaver, J. Phys. Chem., 89, 2787 (1985); (c) G. E. McManis, M. N. Golovin, M. J. Weaver, J. Phys. Chem., 90, 6563 (1986); (d) R. M. Nielson, G. E. McManis, M. N. Golovin, M. J. Weaver, J. Phys. Chem., 92, 3441 (1988); (e) R. M. Nielson, G. E. McManis, L. K. Safford, M. J. Weaver, J. Phys. Chem.,

93, 2152 (1989); (f) R. M. Nielson, M. J. Weaver, J. Electroanal. Chem., 260, 15 (1989). (g) G. E. McManis, R. M. Nielson, A. Gochev, M. J. Weaver, J. Am. Chem. Soc., in press. (h) R. M. Nielson, G. E. McManis, M. J. Weaver, J. Phys. Chem., submitted.

12. G. E. McManis, A. K. Mishra, M. J. Weaver, J. Chem. Phys., 86, 5550 (1987).

13. (a) N. Sutin, Prog. Inorg. Chem., 30, 441 (1983); (b) G. M. Brown, N. Sutin, J. Am. Chem. Soc., 101, 883 (1979); (c) J. T. Hupp, M. J. Weaver, J. Electroanal. Chem., 152, 1 (1983); (d) T. T-T. Li, M. J. Weaver, C. H. Brubaker, J. Am. Chem. Soc., 104, 2381 (1982).

14. (a) B. L. Tembe, H. L. Friedman, M. D. Newton, J. Chem. Phys., 76, 1490 (1982); (b) M. D. Newton, N. Sutin, Ann. Rev. Phys. Chem., 35, 437 (1984).

15. (a) J. N. Onuchic, D. N. Beretan, J. Phys. Chem., 92, 4818 (1988); (b) D. N. Beretan, J. N. Onuchic, J. Chem. Phys., 89, 6195 (1988).

16. (a) M. D. Newton, Int. J. Quant. Chem. Quant. Chem. Symp., 14, 363 (1980); (b) M. D. Newton, J. Phys. Chem., 92, 3049 (1988); (c) Exponential H_{12}-r behavior is not, however, always expected; see: J. Logan, M. D. Newton, J. Chem. Phys., 78, 4086 (1983).

17. Equation (4) is sometimes written in a similar form, but with the electronic matrix elements expressed as linear rather than squared terms (e.g. ref. 16). The present, squared, form is utilized here since for nonadiabatic processes, $\kappa_{el} \propto H_{12}^2$,[16] so that the coefficient α in Eq. (4) describes the decrease in κ_{el} with increasing r (see text).

18. For example: (a) S. Mayo, W. Ellis, R. Crutchley, H. B. Gray, Science, 233, 948 (1986); (b) G. McLendon, Acc. Chem. Res., 21, 160 (1988); (c) K. W. Renfield, J. R. Miller, M. N. Paddon-Row, E. Cotsaris, A. M. Oliver, N. S. Hush, J. Am. Chem. Soc., 109, 5061 (1987); (d) T. T-T. Li, M. J. Weaver, J. Am. Chem. Soc., 106, 6107 (1984).

19. For example: J. Ulstrup, "Charge Transfer Processes in Condensed Media", Springer, Berlin, 1979, Chapter 5.

20. (a) R. A. Marcus, J. Chem. Phys., 24, 966 (1956); (b) R. A. Marcus, J. Chem. Phys., 43, 679 (1965); (c) R. A. Marcus, Ann. Rev. Phys. Chem., 15, 155 (1964).

21. (a) M. J. Powers, P. J. Salmon, R. W. Callahan, T. J. Meyer, J. Am. Chem. Soc., 98, 6731 (1976); (b) M. J. Powers, T. J. Meyer, J. Am. Chem. Soc., 100, 4393 (1976); (c) For a review, see: A. Haim, Prog. Inorg. Chem., 30, 273 (1983).

22. G. E. McManis, M. J. Weaver, J. Chem. Phys., 90, 912 (1989).

23. H. Kramers, Physica, 7, 284 (1940).

24. (a) S. Okuyama, D. W. Oxtoby, J. Chem. Phys., 84, 5824 (1986); (b) S. Okuyama, D. W. Oxtoby, J. Chem. Phys., 84, 5830 (1986).

25. (a) S. A. Adelman, J. Chem. Phys., 64, 124 (1976); (b) S. A. Adelman, B. J. Garrison, Mol. Phys., 33, 1671 (1977).

26. Note that the form of Eq. (13) differs somewhat from expressions given earlier (e.g. refs. 3,4,12); the latter are incorrect.[22] (We are indebted to Dr. Marshall Newton for bringing the correct formulation to our attention.)

27. M. Morillo, R. E. Cukier, J. Chem. Phys., 89, 6736 (1988).

28. S. G. Cristov, "Collision Theory and Statistical Theory of Chemical Reactions", Lecture Notes in Chemistry, Springer-Verlag, Berlin, 1980, Chapter III.

29. (a) V. Levich, R. R. Dogonadze, Coll. Czech. Chem. Comm., 26, 193 (1961); (b) N. R. Kestner, J. Logan, J. Jortner, J. Phys. Chem., 78, 4148 (1974).

30. (a) J. E. Straub, B. J. Berne, J. Chem. Phys., 87, 6111 (1987); (b) Also see related discussion in J. N. Onuchic, P. G. Wolynes, J. Phys. Chem., 92, 6495 (1988).

31. W. H. Press, B. P. Flannery, S. A. Tenkolsky, W. T. Vetterling, "Numerical Recipes", Cambridge University Press, Cambridge, U.K., 1986, p. 126-130.

32. The "inertial limit" is predicted on the basis of the Kramers[23] and related solvent friction treatments (e.g. ref. 6) to provide a maximum rather than a plateau in the rate-τ_L^{-1} (more generally rate-η^{-1}) plots, i.e. the rate is predicted to decrease again for very low friction.[1a,b] Indeed, such a behavior is seen for the present log k_{ex} - log τ_L^{-1} plots derived using Eqs. (9)-(16). However, this "Kramers turnover" is predicted here to occur only at τ_L^{-1} values ($> 10^{13}$ s^{-1}) that are not accessible under conventional experimental conditions.

33. The present treatment presumes, of course, that k_{ex} is sufficiently smaller than the corresponding diffusion-limited rate constant so that this complication is absent.

34. This is because the contributions to k_{ex} from more distant internuclear geometries will tend to be favored more greatly for spherical rather than linear spatial coordinates since the volume increment for a given distance increment increases with r^2 for the former, yet is independent of r for the latter coordinates.

35. R. M. Nielson, M. N. Golovin, G. E. McManis, M. J. Weaver, J. Am. Chem. Soc., 110, 1745 (1988).

36. (a) J. D. Morgan, P. G. Wolynes, J. Phys. Chem., 91, 874 (1987); (b) L. D. Zusman, Chem. Phys., 112, 53 (1987).

37. P. G. Dzhavakhidze, A. A. Kornyshev, L. I. Krishtalik, J. Electroanal. Chem., 228, 329 (1987).

38. For example: (a) P. Siders, R. J. Cave, R. A. Marcus, J. Chem. Phys., 81, 5613 (1984); (b) R. P. Dominque, M. D. Fayer, J. Phys. Chem., 90, 5141 (1986).

39. G. E. McManis, M. J. Weaver, J. Chem. Phys., 90, 1720 (1989).

40. H. Frauenfelder, P. G. Wolynes, Science, 229, 337 (1985).

41. Note that Eq. (9) in ref. 12 contains a typographical error, in that the factor of 4 in the numerator (within the square root) should instead be placed in the denominator.

Figure Captions

Fig. 1

Logarithmic plots of the calculated rate constant for electron self exchange, k_{ex} ($\underline{M}^{-1}$ s^{-1}), against the inverse longitudinal solvent relaxation time, τ_L^{-1}, for various values of the electronic coupling matrix element, H_{12}. Values of k_{ex} calculated using the simplified expression for k_{et} [Eq. (23)] along with Eqs. (1), (4)-(6). The values of H_{12} at reactant contact, H_{12}^o, are 0.02, 0.05, 0.1, 0.2, 0.5, and 1.0 kcal mol^{-1}, corresponding to progressively increasing k_{ex} values. Other parameters used in these calculations are $\Delta G_c^* = 5.0$ kcal mol^{-1}, $\alpha = 1.25$ $Å^{-1}$, $r_o = 2a = 8$ Å, and $T = 298$ K.

Fig. 2

As in Fig. 1, except that k_{et} is calculated using the more complete expression [Eq. (27)], with k^{TST} given by Eq. (18), $\tilde{\kappa}_{el}$ from Eq. (20), and k_{et}^a from Eqs. (8)-(16). Values of $\omega_o/2\pi$ taken to be 1×10^{12} s^{-1} and 5×10^{12} s^{-1} in Figs. 2A and 2B, respectively.

Fig. 3

Comparisons between log k_{ex} - log τ_L^{-1} plots calculated by using spatial integration of k_{et} (solid, dotted curves) with those obtained from the simplified encounter preequilibrium treatment (dashed curves). The lower and upper sets of curves refer to H_{12}^o values of 0.05 and 0.5 kcal mol^{-1}, respectively. The solid curves were calculated exactly as in Fig. 2B, and the dotted curves as in Fig. 1. The dashed curves were calculated using k_{et} values obtained as for the corresponding solid curves, but by inserting k_{et} for $r = r_o$ (= 8 Å) into the encounter preequilibrium expression [Eq. (7)], with K_p taken as 0.25 $\underline{M}^{-1}$ (see text).

Fig. 4

Plots of k_{et} normalized to the value with reactants in contact, k_{et}/k^{o}_{et}, against the radial separation distance, $(r - r_o)$. Values of k_{et} calculated as noted in caption to Fig. 2B. Each trace refers to the different H^{o}_{12} values, as indicated (kcal mol^{-1}). Values of τ_L fixed at 5×10^{-8} s and 5×10^{-12} s in Figs. 4A and B, respectively.

Fig. 5

As in Fig. 4A, but calculated with ΔG^{*}_{c} value held independent of r.

Fig. 6

Comparisons between log k^{e}_{ex} - log τ_L^{-1} plots for electrochemical exchange calculated by using spatial integration of k_{et} (solid, dotted curves) with those obtained using the encounter preequilibrium treatment (dashed curves) (cf Fig. 3 for homogeneous bimolecular case). The lower and upper sets refer to H^{o}_{12} values of 0.05 and 0.5 kcal mol^{-1}, respectively. The solid curves take into account the effects of barrier top roundedness and the inertial limit upon k_{et} using Eq. (27), along with Eqs. (8-16), (18), and (20). The parameters used are: $\Delta G^{*} = 5.0$ kcal mol^{-1} [for $r_e = \infty$, Eq. (6a)], $\alpha = 1.25$ $Å^{-1}$, $r_o = 2a = 8$ Å, $\omega_o/2\pi = 5 \times 10^{12}$ s^{-1}, and T = 298 K. The dotted curves were calculated using Eq. (23) in place of Eq. (27). The dashed curves were calculated using k_{et} values obtained as for the corresponding solid curves, but by inserting k_{et} for $r_e = r_o$ (= 8 Å) into the encounter preequilibrium expression [Eq. (7)], with K_p taken as 0.5 Å (see text).

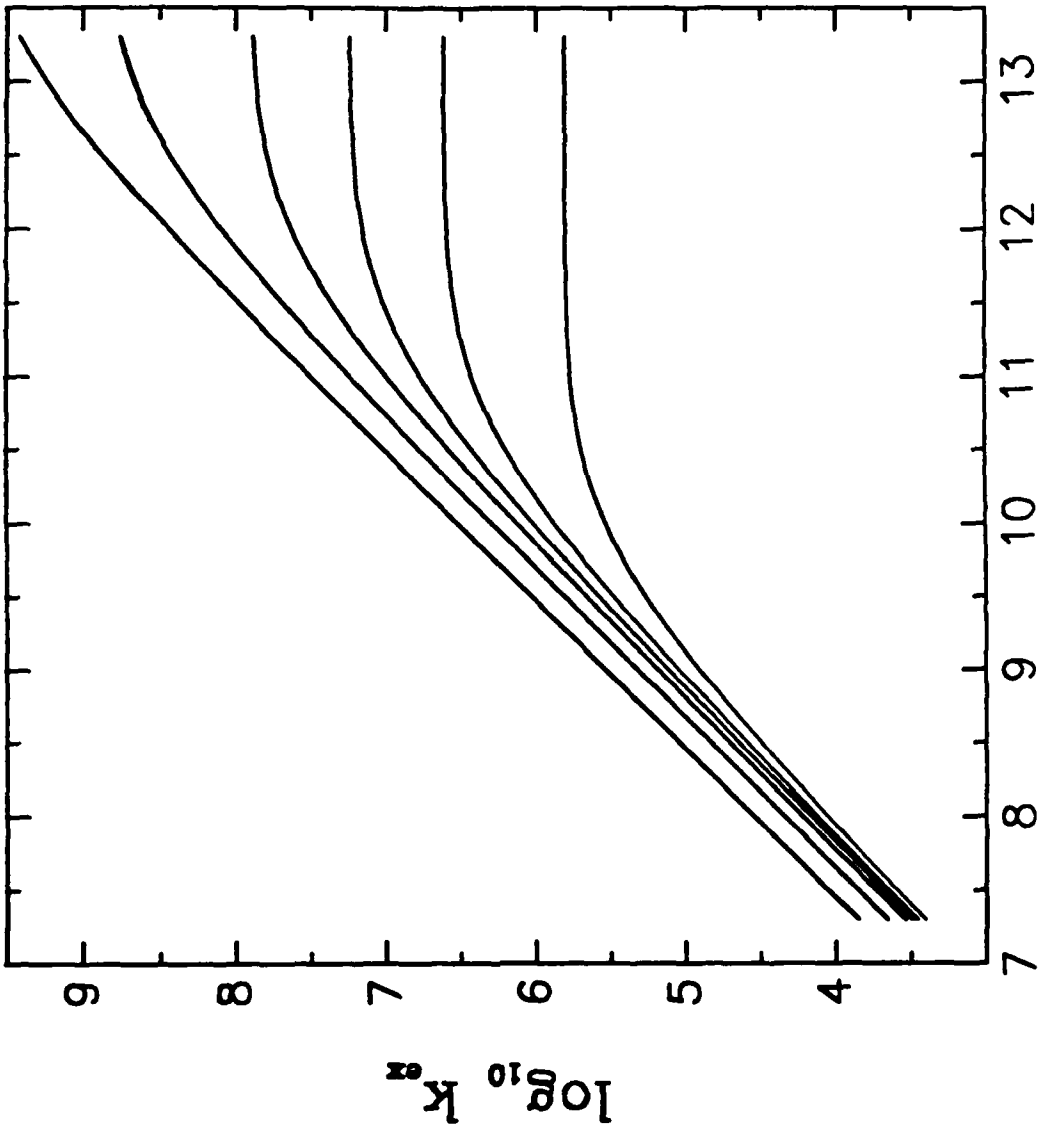

GOCHEV ET AL

FIG 1

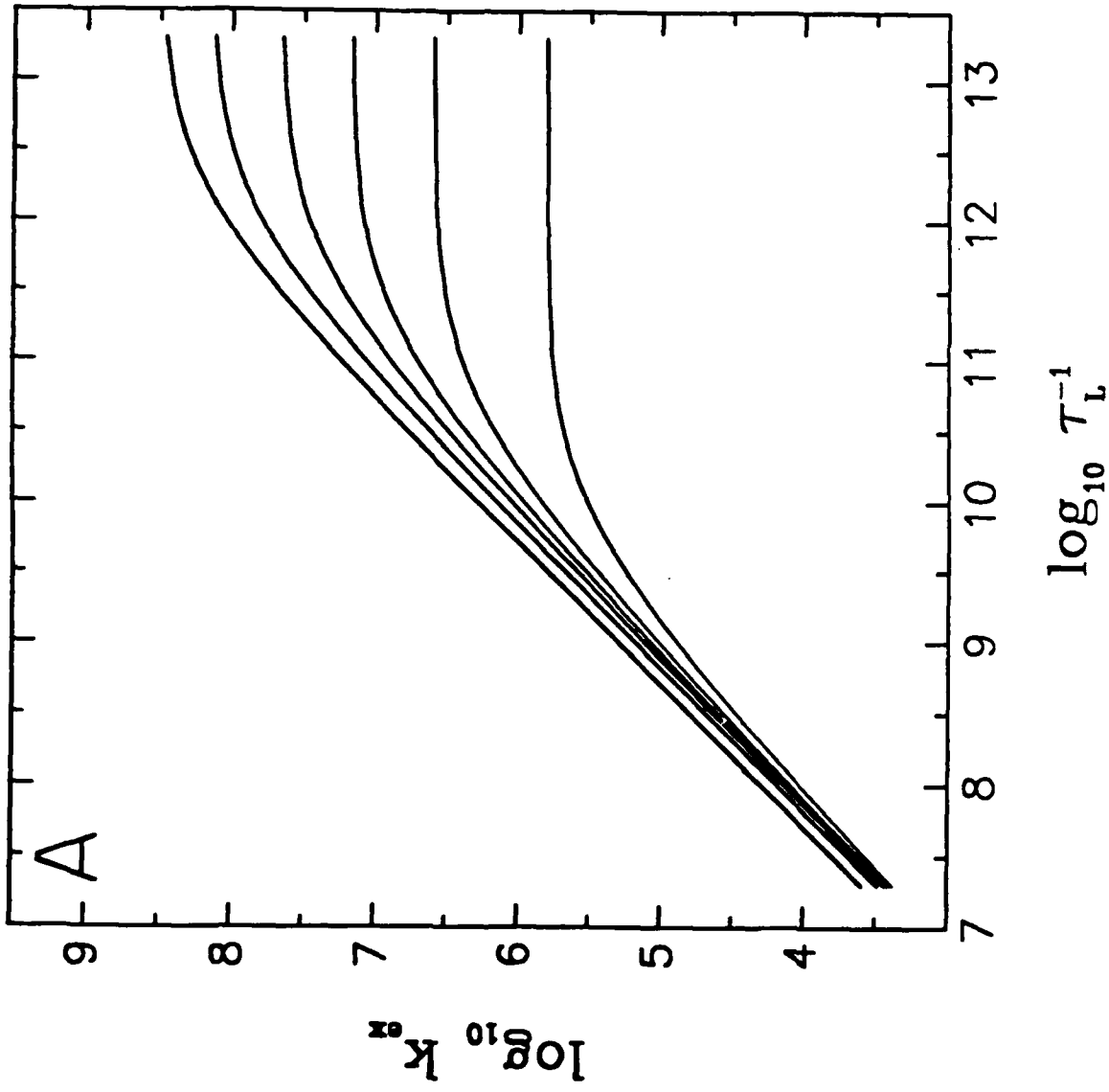

GOCHEV ET AL

FIG 2A

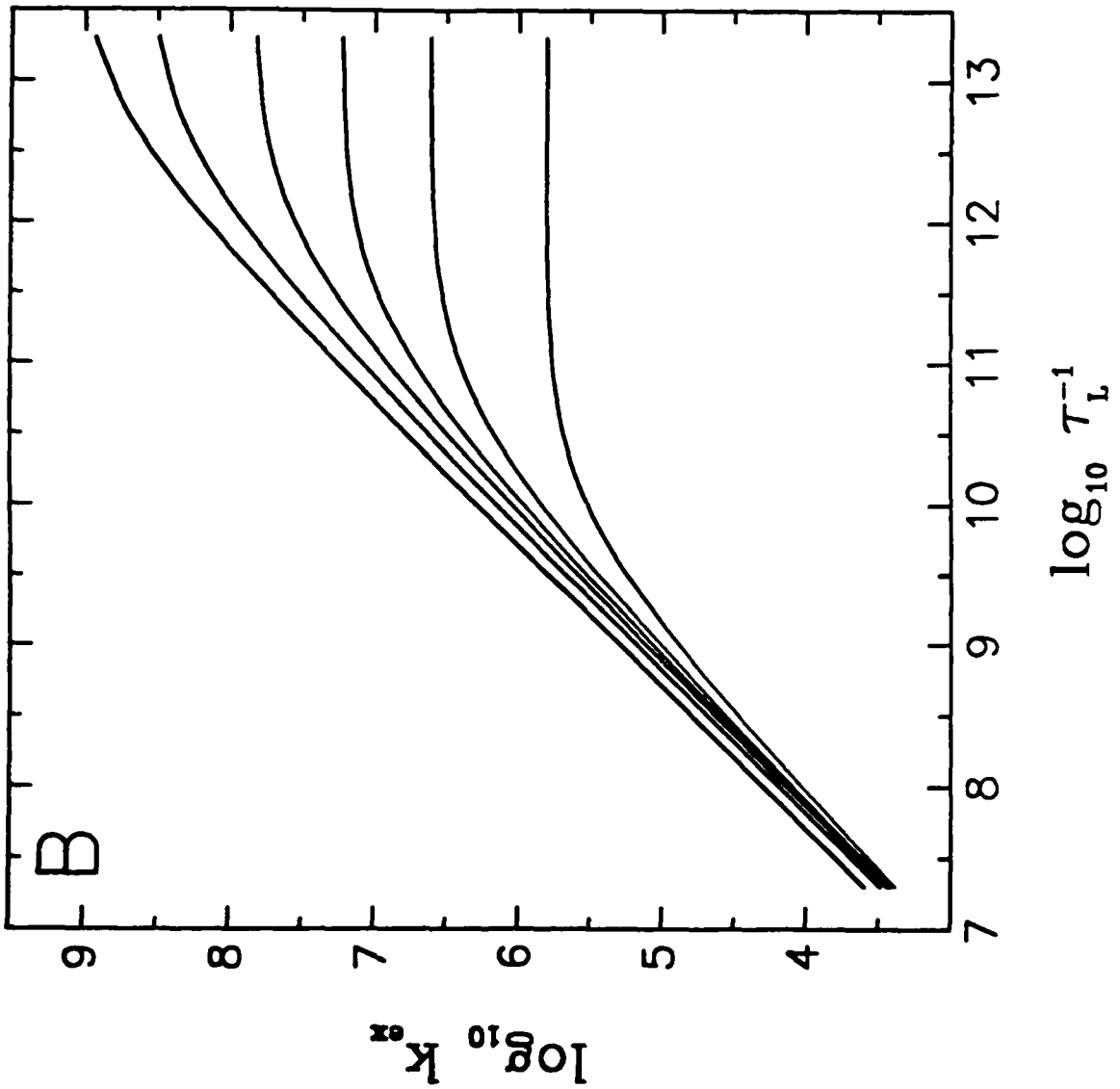

GOCHEV ET AL

FIG 2B

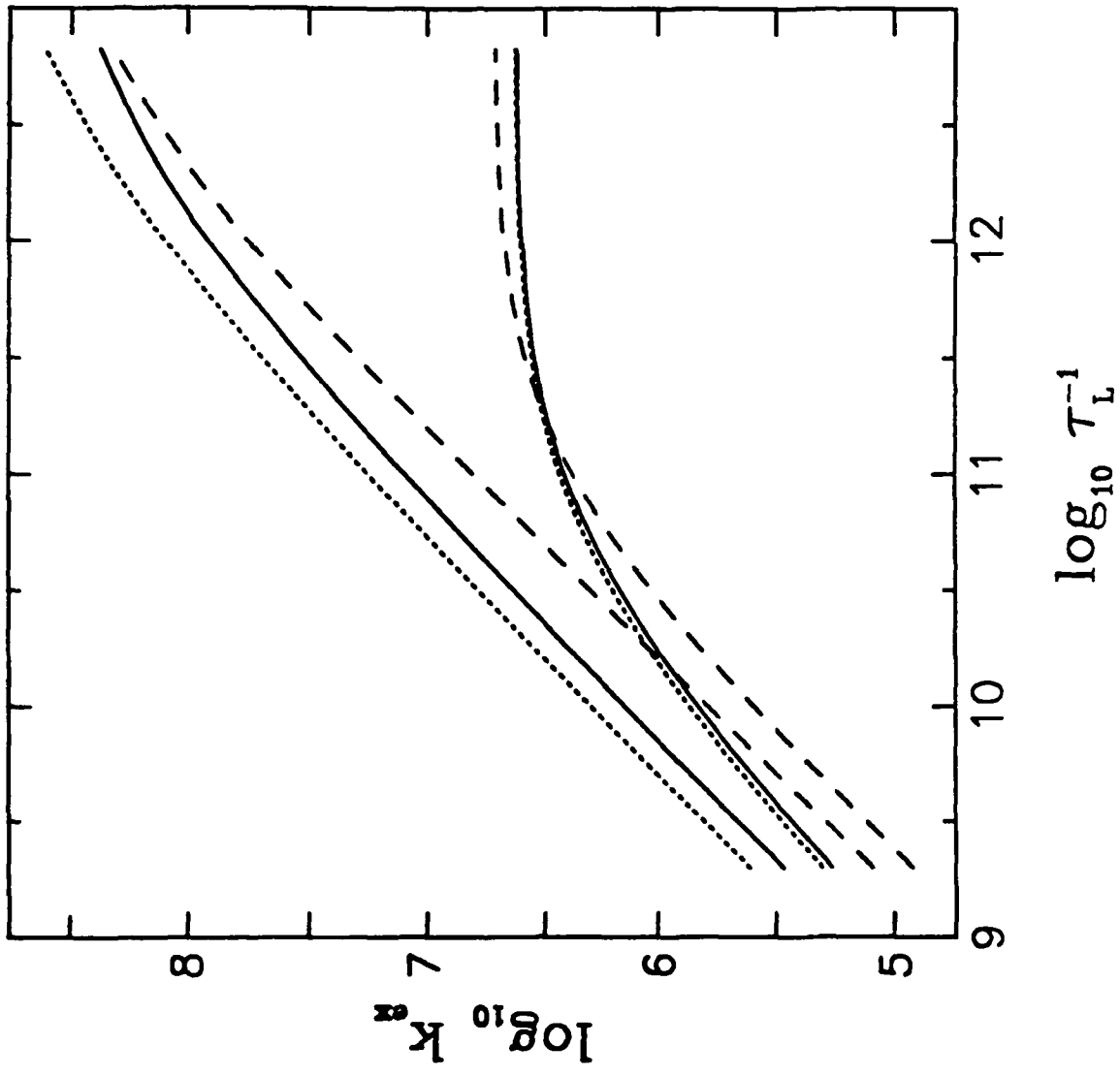

GOCHEV ET AL

FIG 3

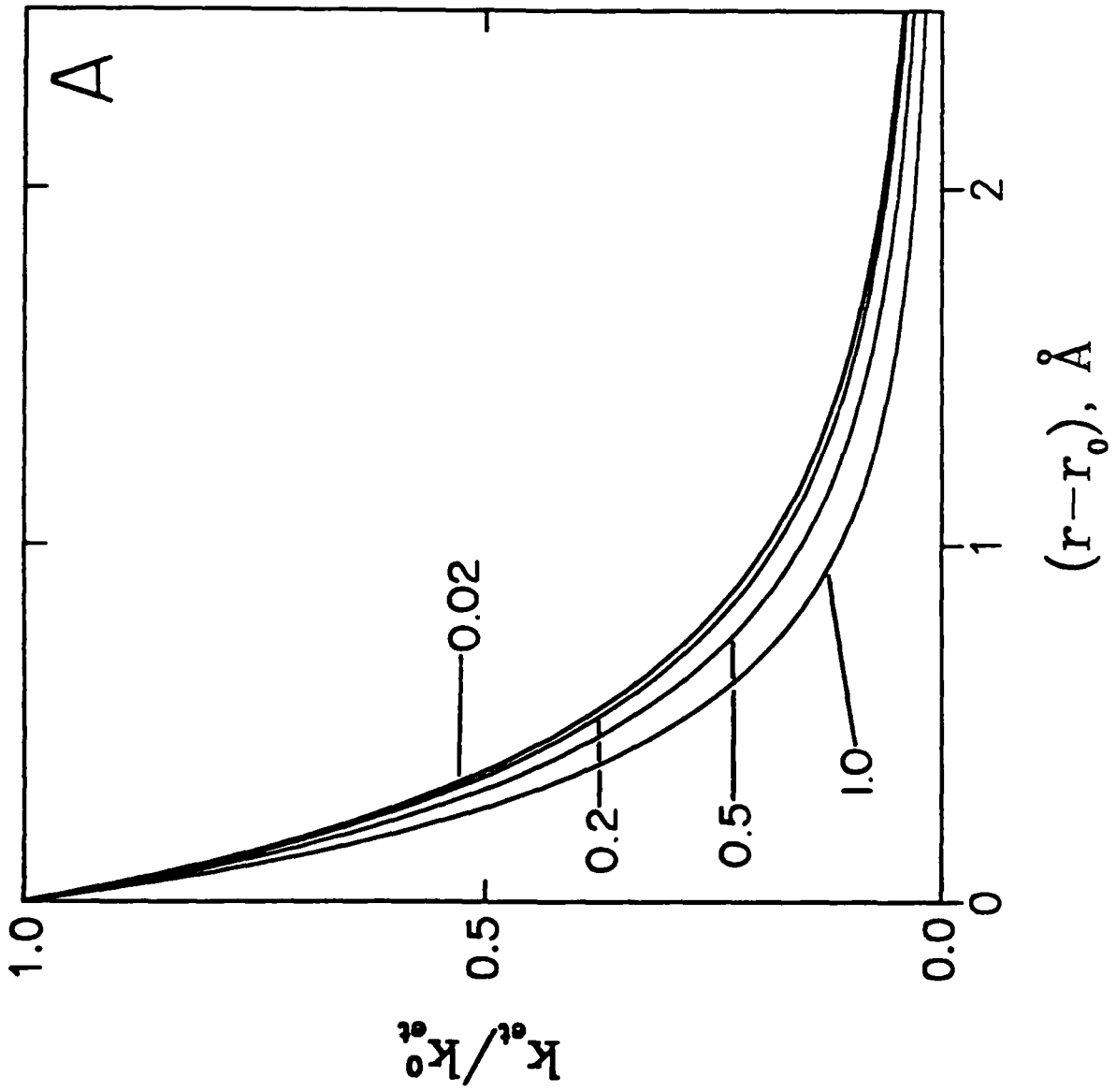

GOCHEV ET AL

FIG 4A

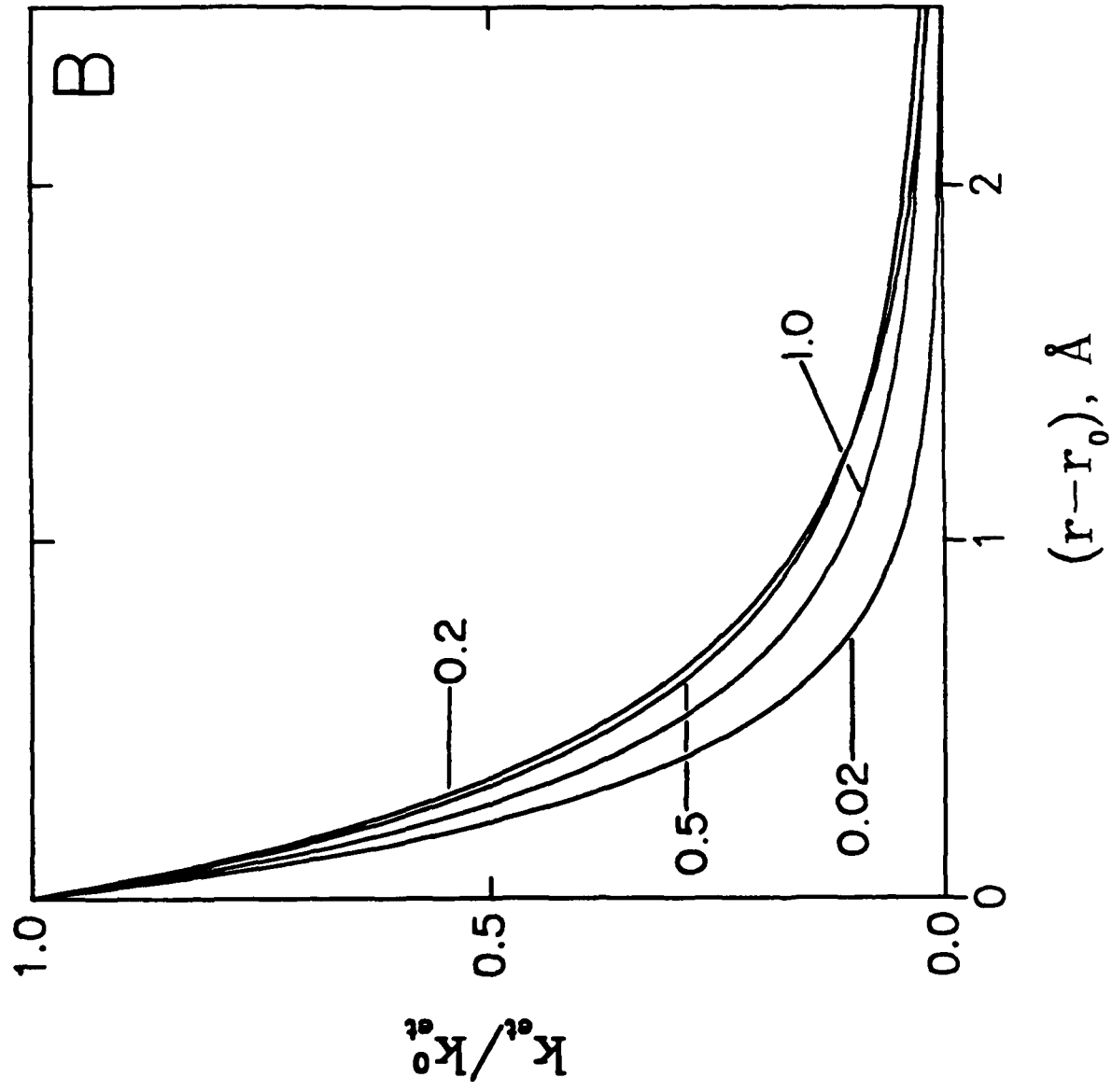

GOCHEV ET AL

FIG 4B

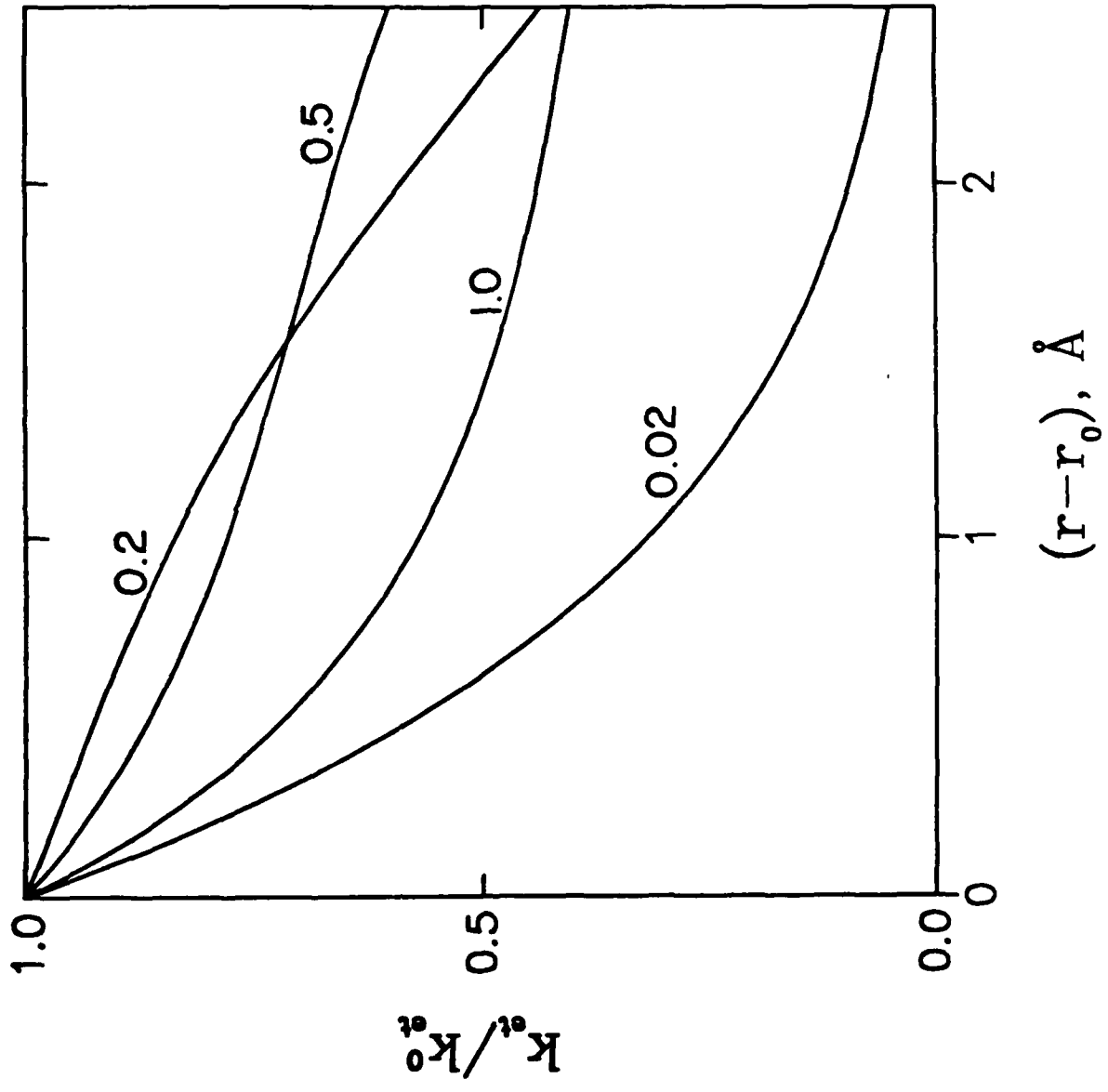

GOCHEN ET AL

FIG 5

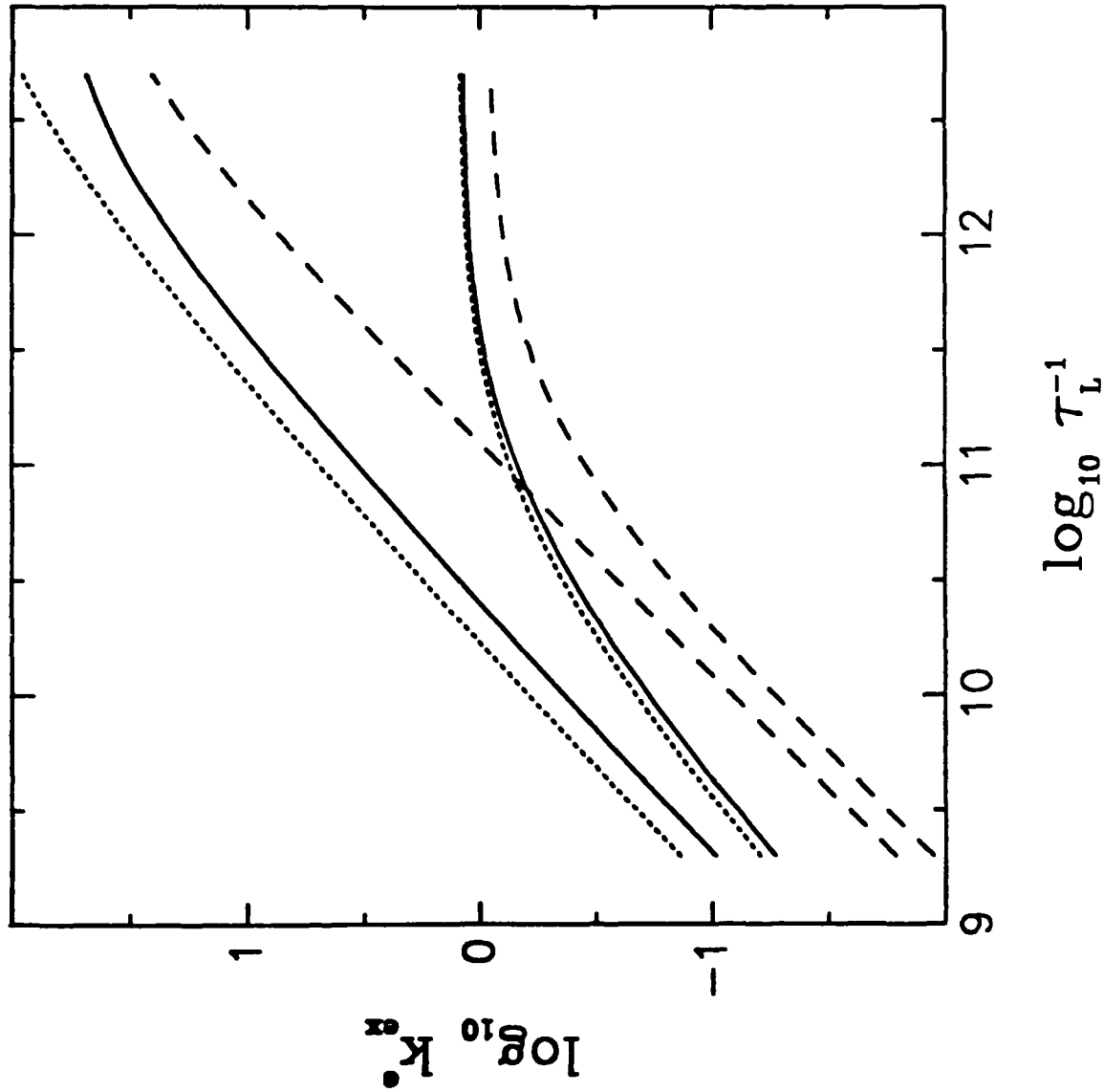

GOCHEV ET AL

FIG 6